IS-T--981

DE82 005450

MASTER

Diffusion in Calcium Oxide/Calcium Sulfate Pellets

by

Kou-Liang Chang

M.S. Thesis submitted to Iowa State University

Ames Laboratory, U.S. DOE

Iowa State University

Ames, Iowa 50011

Date Transmitted: October 1981

PREPARED FOR THE U. S. DEPARTMENT OF ENERGY

UNDER CONTRACT NO. W-7405-Eng-82.

DISCLAIMER

DISCLAIMER

Printed in the United States of America

Available from
National Technical Information Service
U.S. Department of Commerce
5265 Port Royal Road
Springfield, VA 22161

Diffusion in calcium oxide/calcium sulfate pellets

by

Kou-Liang Chang

A Thesis Submitted to the

Graduate Faculty in Partial Fulfillment of the

Requirements for the Degree of

MASTER OF SCIENCE

Major: Chemical Engineering

Approved:

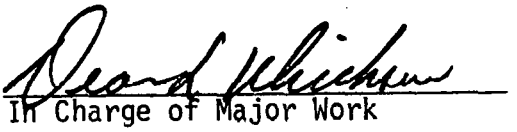

In Charge of Major Work

For the Major Department

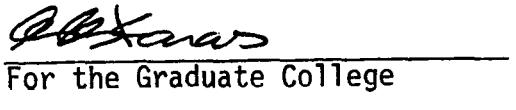

For the Graduate College

Iowa State University
Ames, Iowa

1981

TABLE OF CONTENTS

LIST OF TABLES

LIST OF FIGURES

NOMENCLATURE

A	cross-sectional area of the pellet, cm^2
$A\phi$	rate constant in the rate equation for sintering
C_A	concentration of the tracer in the pore volume, $mole/cm^3$
C_{AL}	concentration of the tracer at X = L, $mole/cm^3$
CO	calcium oxide
CS	calcium sulfate
D	molecular diffusion coefficient of gaseous reactant, cm^2/sec
D_{AB}	binary molecular diffusivity of gaseous species A and B, cm^2/sec
D_{AC}	binary molecular diffusivity of gaseous species A and C, cm^2/sec
D_e	effective diffusivity of species A in the pellet, cm^2/sec
D_{EA}°	initial effective intergrain diffusivity, cm^2/sec
D_{KA}	Knudsen diffusion coefficient for gaseous species A, cm^2/sec
E_S	activation energy for the sintering process
F	volumetric flow rate through lower chamber, cm^3/sec at P = 1 atm and t = 24°C
g	stoichiometric factor of the solid product
g_2	r_g/r_{go}
L	pellet length, cm
M	molecular weight, gm
M_n	nth moment about the origin, defined as $M_n = \int_o^\infty Ct^n dt$
N_d	No. of solid grains per unit volume of porous solid, $N_d = 3\,(1-\varepsilon)/4\pi rg$
P	pressure, atm

ro initial radius of pellet, cm

r_g grain radius, $r_g = r_{go} [1 + (\phi-1) X]^{1/3}$, cm

r_{go} initial grain radius, 3×10^{-4} cm for CaO pellet

R radial distance in the pellet, cm; gas constant, 8.314×10^7 $gcm^2/°K\ sec^2$

Rg gas constant

S Laplace variable, S^{-1}

t time, sec

t_o injection time of pulse, sec

T temperature, ^oK

Tc Tamman temperature, corresponding to the onset of sintering, ^oC

V_1, V_3 volume of upper and lower chambers, cm^3

X coordinate in direction of diffusion in pellet, cm

X conversion ratio

y_1 initial weight of CaO pellet, gm

y_2 final weight of CaO pellet, gm

y_A mole fraction of species A in gas mixture

Y overall conversion

Greek letters:

ε local pellet porosity

ε_o initial pellet porosity

ε_p total pellet porosity

$\delta(t)$ dirac delta pulse, sec^{-1}

τ pellet tortuosity

τ_o initial pellet tortuosity

ϕ expansion coefficient, 2.72 for CaO sulfation system

α function of flux ratio, $\alpha = 1 - (\frac{M_A}{M_B})^{\frac{1}{2}}$

μ_1 first absolute moment, $^{m_1}/_{m_o}$, sec

ρ density of the reacted pellet, gm/cm^3

σ_{AC} collision diameter of species A and C, cm

$\Omega_{D,AC}$ dimensionless function of the temperature and of the intermolecular potential field for one mole of A and one of C

ABSTRACT

Diffusion rates in calcium oxide pellets after partial conversion to calcium sulfate were measured. A Wicke-Kallenbach type diffusion cell operated in the pulse-response mode was used to measure effective diffusivity.

Cylindrical calcium oxide pellets were formed from the powder using pelletizing pressures of 10,000, 20,000 and 30,000 psi. The pellets were reacted at 325, 500 and 600°C with sulfur dioxide and oxygen to form calcium sulfate. The volume of calcium sulfate is 2.7 times that of calcium oxide, so partial pore closure occurs. The diffusivity was measured in the original pellet and in pellets partially reacted to several different conversion levels.

The effective diffusivity decreases as conversion decreases and is roughly inversely proportional to pellet porosity squared for low conversions. However, the porosity and diffusion rate do not become zero when the reaction rate approaches zero. Pore closure is, therefore, not the mechanism which limits the ultimate conversion. A large diffusion resistance through the calcium sulfate product layer probably causes the reaction to stop before total conversion.

The final conversion obtainable increases as reaction temperature increases and decreases as pelletizing pressure increases.

I. INTRODUCTION

Gas-solid reactions play a major role in the technology of most industrialized nations and are frequently encountered in the process industry, e.g., in coal gasification, in ore processing, iron production, and roasting of pyrites. Work in this field has become prominent during the past three decades. For gas-solid reactions, the conditions inside the particle change with time because the solid itself is involved in the reaction, and the solid matrix through which diffusion is taking place may undergo changes during the process. Thus, despite a considerable amount of work, the wide variations in pore structure in terms of pore shapes, pore sizes and interconnection of pores has prevented development of a satisfactory geometric model of general applicability. These variations in structure are not sufficiently well-defined by structural indices commonly available, such as mean pore size, surface area and pore volume. Understanding the influences of the detailed structure would be of considerable help in interpreting the results of diffusion experiments and in predicting the effective surface area available for reaction within the pellet.

Several mathematical models have been developed to quantitatively describe gas-solid reactions. These models can usually be categorized into two general types. The grain models postulate the solid reactant to exist in small grains uniformly dispersed within a solid pellet (18, 33, 35, 36, 37). The pore models consider the solid reactant to be semi-infinite and contain a combination of macro-pores and micro-pores

(10, 17, 24, 40, 44).

In addition, a few diffusion models are available for predicting the gaseous diffusion rate in porous systems (6, 12, 13, 37). However, prediction of the effective diffusivity in porous solids undergoing reaction is still uncertain, partly because the diffusion flux may include a contribution from several mechanisms including bulk, Knudsen and surface diffusion. In particular, very little is known about surface diffusion and rates of transport by this mechanism. Moreover, no one technique for measuring diffusivities in porous solids is perfect. Since careful and detailed experimentation is seriously lacking, for example, few investigators of gas-solid reactions have carried out independent measurement of even a single gas diffusivity within their solid and even fewer have done so at reaction conditions, it would be hard to assess these models as to their respective merits.

The two major methods of measuring diffusion coefficients are steady state and unsteady state methods. The steady state method is based on steady-state countercurrent diffusion flux measurements under zero pressure gradient. The method is time consuming and suffers from several disadvantages; for example, diffusion into dead-end pores goes undetected although such pores play a part in gas-solid reactions. The unsteady state method gives values which include appropriate contributions from micropores and dead-end pores. It is simple to carry out and can be conveniently used over a wide range of temperatures. However, it has some shortcomings as applied to calculation of effectiveness factor which do not appear to be always appreciated.

The object of this study is to extend the dynamic method, reported by Smith based upon the Wicke-Kallenbach diffusion cell (32), for measuring the diffusivities in porous solids. In particular, the diffusion measurements are to be made at several conversion levels of solid to determine how solid conversion affects the diffusion rate. These results will help determine the intricate relationships among conversion ratio, porosity, diffusivity, and other physical properties.

The chemical reaction between calcium oxide and sulfur dioxide at high temperature in the presence of excess oxygen (4, 18) is:

$$CaO + SO_2 + \frac{1}{2} O_2 \longrightarrow CaSO_4$$

Borgwardt (3) found that the reaction was of first order with respect to sulfur dioxide, and that the rate of reaction decreased rapidly as solid conversion increased. During the first few minutes of exposure, the sulfation occurs almost entirely in the outer parts of the particle, but as time continues, this reaction zone gradually spreads through the particle interior. However, a concentration gradient of sulfate persists within the particles even after long exposure times. In the advanced stage of the reaction, a dense shell of the reaction product exists at the outer surface of the particles and closes some of the pores so that the overall process is then governed by transport of sulfur dioxide through the remaining pores.

II. LITERATURE REVIEW

A. Measurement of Diffusion Coefficients

1. Some models of gas diffusion in porous media

There are a number of simplified models of porous media which permit mathematical description. A good model at best would predict diffusion constants from known properties of gases and porous materials or, at least, it would enable one to transfer results obtained with one system to another (similar) one. Work described in the literature is usually concerned with only one model at a time; in the majority of cases only one pair of gases with simple structure has been used. Obviously, different models require different amounts of information concerning the properties of the system; in the diffusion equations, therefore, different numbers of constants appear.

The model of Johnson and Stewart (20) is based on the idea that a porous medium can be described by a bundle of parallel oriented cylindrical capillaries with different radii. Their essential work dealt with the effects of pore-size distribution and pore orientation on diffusion rates. Surface diffusion was neglected. For simplicity, only isothermal, isobaric conditions were compared in the theory as well as in the measurements. Using this model, which is called the parallel path pore model also, it is possible to either predict the diffusion flux or to calculate tortuosity from experimentally determined fluxes.

Wakao and Smith proposed a random pore model (42) that divides the

pores into micropores and macropores and represents the diffusion flux as being the sum of that through the macropores, that through the micropores and that by a series diffusion path through both. To apply the model requires a knowledge of the pore volume and pore radius distribution for the porous material. The experimental diffusion measurement results showed that the model predicts rates in good agreement with the data over the pressure range investigated 1-12 atm.

Brown et al. (6) used the parallel path model and the Wakao and Smith (42) model to predict diffusion rates over the pressure range 1-20 atm, using 12 porous materials with widely different pore-size distributions. For the material reported by them, there appeared to be little choice between the absolute predictive capabilities of these two models. In addition, two of the conclusions of the Sattlerfield-Cadle articles (30) are confirmed: the approximate factor of 2 for the predictive ability of the parallel path model with an occasional exception; and the superior capability of the parallel path pore model in extrapolating data from one pressure to another.

The Dusty-gas model was presented by Evans et al. (14) for the diffusion of gases in porous media in the absence of pressure gradients in which the porous medium is visualized as a collection of uniformly distributed dust particles which are constrained to be stationary. By formally considering the dust particles as giant molecules, it is possible to derive all the desired results simply from rigorous kinetic theory as special cases of multicomponent mixtures. By formally varying the mole fractions of the real gas molecules, the entire pressure range

from the Knudsen region to the normal diffusion region can be covered. The model predicts that the flux ratio for binary mixtures is equal to the inverse square root of the ratio of molecular weights at all pressures. It also gives a rigorous theoretical treatment of the entire transition region, from which one can obtain the Bosanquet interpolation formula and a differential equation for diffusion which covers the entire range. Ran and Robert proposed the extended dusty-gas model (25) being used to describe the transport for a zero-order, irreversible reaction with mole changes. Results agree with other models in the purely Knudsen and molecular regimes. In the transition region, however, the effectiveness factor is a function of five dimensionless parameters. Rinker and Chen (27) modified the dusty-gas model and used volume-mean correction factors in the model to account for heteroporosity effects on isobaric and nonisobaric mass transfer in general porous media. The modified model describes isobaric diffusion in T-126 alumina pellets considerably better than the original model.

The particle-pellet model was proposed by E. Calvelo and J. M. Smith (8), in which the pellet was formed by compressing nonporous, reactant particles. In such a system, both intrapellet diffusion and reaction resistances can be significant. This model has considerable flexibility since simplifying assumptions can be made independently for particle and pellet. This allows a reasonably facile treatment for nonisothermal conditions. With this model, instability can be considered for the more general situation of reaction and diffusion

over a region.

2. The techniques for measuring diffusivities in porous media

Diffusion rates in solid pellets are necessary for design of many types of reactors. Prediction methods based upon the geometrical properties of the porous pellet are available, but their accuracy is about 50 to 100% (32), hence, experimental methods are needed. Several experimental techniques have been used for the determination of effective diffusion coefficients of gases and vapors in porous solids and can be broadly divided into steady and unsteady-state methods.

Wicke and Kallenbach (43) designed a steady-state method which is now used for pellets with regular geometry. The overall effective diffusion coefficient is determined from the known dimensions of the pellet, concentration difference, and diffusion rate. The attraction of the method is that it gives a direct measurement of effective diffusion coefficient, unlike some other methods in which the diffusion coefficients are indirectly calculated in the presence of complicating factors. However, because the flux equations make no allowances for the presence of dead-end pores, the experimental results may give misleading values. If the solid has a small fraction of pore volume in relatively large interconnected pores, most of the flux would be through these pores and finer pores, containing most of the surface area, would contribute very little. For these reasons, the application of steady-state diffusion coefficients to reaction may not be correct since the reactants will have to diffuse to small pores where most of the solid

area lies and where diffusional resistance is also great. In such circumstances the diffusivities from reaction data can then be expected to be lower than those from steady-state diffusion data.

Unsteady-state methods (dynamic methods) based on transient diffusion flux measurement give effective diffusivities which account for micropores and dead-end pores in the solid. The most popular technique is based on a chromatographic technique which utilizes the broadening of a pulse of tracer gas as it passes through the packed bed of pellets. Van Deemter et al. (41) developed an elementary plate theory of mass transport in a packed chromatographic column to relate the pulse dispersion and retention time to the mass transport parameters in the column. Trimm and Corrie (39) determined the effective diffusivities of oxygen, nitrogen, and butadiene in tin-antimony oxide catalysts using the chromatographic method and applying Van Deemter's theory. They found unsteady-state values about 20% higher than steady-state values and attributed this to the influence of dead-end pores. Experimental measurements of the dynamic method are fast and simple enough to be used as a standard routine procedure in laboratories.

A dynamic method for catalyst diffusivities was proposed by Smith and co-workers (7, 13, 32). He showed that a pulse-response technique could be used with a Wicke-Kallenback type of diffusion cell to determine effective diffusivities in catalyst pellets. The diffusivity was a function of the retention time of the pulse of diffusing gas in the pellet. Other quantities involved were the porosity, length, cross-sectional area of the pellet, and the flow rate of gas across the face of the pellet. For

very large values of flow rate, the expression for effective diffusivity was simplified to one requiring only the retention time, porosity, and length of the pellet. The method was evaluated with experimental data at 24°C and one atmosphere for the diffusion of helium (in nitrogen) in an alumina pellet of 0.48 porosity. The results indicated that an accurate value of effective diffusivity could be obtained. The apparatus was simple and the time required was short so that the procedure could be attractive for use on a routine basis in catalyst laboratories.

B. The Effect of Conversion in Gas-solid Reaction Systems

Ulrichson and Yake (40) have developed a two-dimensional expanding grain model that accounts for bulk flow which was successfully applied to the lime chlorination system. The solid-gas reaction between CaO and Cl_2 has been studied in a series of experiments employing thermogravimetric analysis, with varying temperature, pellet size, and chlorine concentration. Since the reaction is an example of a class of irreversible gas-solid reaction systems that exhibits dramatic structural changes with reaction due to an expanding product layer and that is characterized by a net consumption of gas, the expanding grain model that allows for bulk flow transport could be used as a basis for analyzing the system. They assumed that the pellet was isothermal and mass transfer resistance in gas phase was negligible, then two-dimensional diffusion equations for an irreversible reaction were used to yield the model applicable to the lime chlorination. For this model, the initial effective diffusivity,

D°_{EA}, was estimated using the following equation:

$$D^{\circ}_{EA} = \frac{1}{\frac{1}{D_{AC}\,\varepsilon_o/\tau_o} + \frac{1}{D_{KA}}} = \frac{1}{\frac{1}{D_{AC}} + \frac{\varepsilon_o^2}{D_{KA}}} \cdot \varepsilon_o^2$$

where ε_o, the initial pellet porosity, was set equal to $1/\tau_o$ in accord with the random pore model, and ε_o was determined experimentally. Consequently, only 3 parameters must be determined from curve fitting the data: K, σ_g^2 and ε_m. The rate constant, K, was obtained from the initial rate data, whereas σ_g^2, Theile-type parameter for the grain, and ε_m, minimum local porosity, could be adjusted to provide the best overall representation of the conversion versus time data.

C. Georgakis et al. (15) studied the SO_2 absorption in calcined dolomites and presented two gas-solid reaction models: the pore plugging model and the expanding grain model. The idea for the pore plugging model is that the pore mouth will plug because of product expansion and the reaction will cease after some time because of the increased diffusion resistance. The model predictions were compared with experimental data obtained by Hartman and Coughlin (17, 18) on the sulfation of uncalcined limestone. It was seen that the model accurately predicted the experimental data. The expanding grain model generalized all previous grain models which were that the grain size was assumed to remain constant during reaction time for the cases that ϕ, expansion coefficient, was not equal to one, by allowing the grain size to change with conversion. They showed that a linear relationship between porosity and conversion existed not only on the average but locally as well. The

time needed to plug the pores at the surface of the pellet was analytically calculated. This permitted an additional insight into the relationship between the diffusion coefficient through the solid product and the intrinsic reaction rate constant. The experimental data obtained by Borgwardt (3) and Borgwardt and Harvey (4) were compared against predictions of the expanding grain model. It appeared the accuracy of the model was quite satisfactory. In this model, the location conversion $Y(R,t)$, which is equal to $[1 - g_2^3(R,t)]$, was related in the following linear fashion to the local porosity $\varepsilon(R,t)$,

$$\frac{1 - \varepsilon(R,t)}{1 - \varepsilon_o} = \phi + (1-\phi)g_2^3(R,t) = \phi + (1-\phi)[1-Y(R,t)]$$

where g_2 is the reaction front distance with respect to the initial pore radius. The relationship was integrated with respect to the pellet volume and a linear relationship relating the average porosity to the overall conversion was obtained.

Ramachandran and Smith (23) proposed a theory to account for the effects of the solid structural changes on the conversion-time relationship and on temperature profiles in the pellet. The theory was based on the particle pellet concept and accounted for differences in density between reactant and product solids and for changes of porosity and pore interconnections due to sintering. The rate of sintering was assumed to obey an Arrhenius-type equation. The effect of structural changes on the effective diffusivity was developed using the results of Kim and Smith (21) who had studied the effect of sintering on the effective

diffusivity in nonreactive systems. The starting point had been the random pore model. However, it was not adequate to account for the effects of sintering. Thus, a more complicated model for the effects of sintering was developed as follows:

$$De = \frac{D}{g(\phi)} [1 - (1-\varepsilon_o)(\frac{r_g}{r_o})^3]^2(1-\phi)^2$$

$$\frac{d\phi}{dt} = (1-\phi)A_\phi \exp [- \frac{E_s}{R_g(T-Tc)}]$$

where the second equation is an Arrhenius-type equation, E_s is the activation energy for sintering, Tc is the Tamman temperature, and $A\phi$ is the rate constant in the rate equation for sintering. From these two equations, the effective diffusivity can be estimated by first estimating values for the model parameters $A\phi$, E_s and Tc from sintering experiments on the product solid.

III. THEORY

A. The Pulse Technique

The pulse technique in the single pellet was first used for diffusion studies by Suzuki and Smith (34), but a modified technique was successfully applied by Dogu and Smith (12) to measure the effective diffusivity for an alumina pellet. Bob Thies (38) used Dogu and Smith's method and set up a computer program to compute the effective diffusivity for the gas-solid raction system of CaO chlorination. In this study, we use the same technique as Bob Thies' for CaO sulfation system. The theory of the pulse technique can be illustrated using figure 1.

For a nonabsorbed gas, the conservation equation applied to a section of the pellet is (refer to Appendix A):

$$\varepsilon_P \frac{\partial C_A}{\partial t} = D_e \frac{\partial^2 C_A}{\partial X^2} \tag{1}$$

$$D_e = \frac{1 - \alpha y_A}{D_{AB}} + \frac{1}{D_{KA}} \tag{2}$$

where D_e has been assumed to be independent of composition as long as the mole fraction y_A approaches zero and the term αy_A in equation 2 can be neglected.

The boundary and initial conditions are:

$$C_A = M\delta(t) \qquad \text{at } X = 0 \tag{3}$$

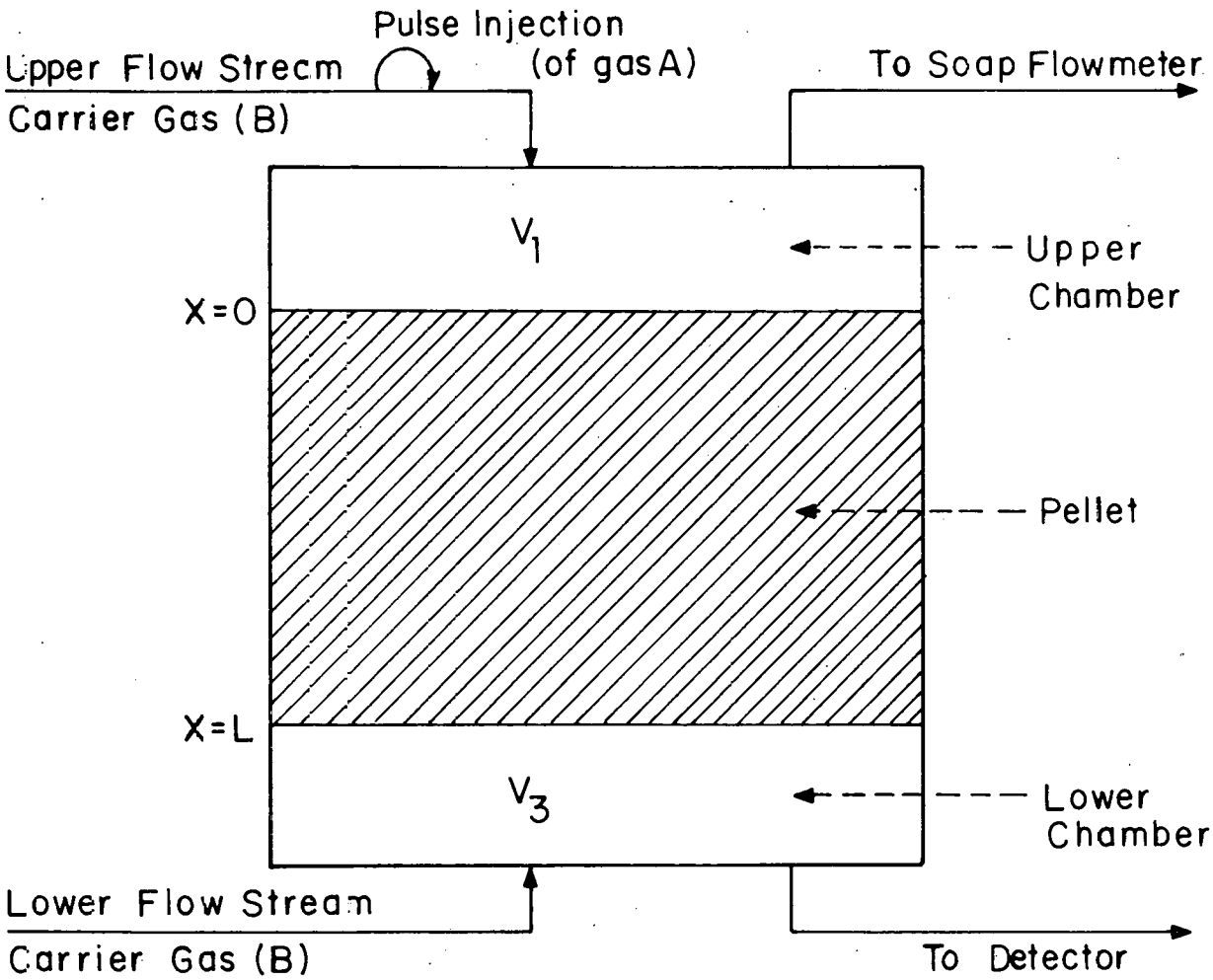

Figure 1. Schematic diagram of the single pellet system

$$AD_e\left(\frac{\partial C_A}{\partial X}\right)_{x=L} = V_3\left(\frac{dC_{AL}}{dt}\right) + F\,C_{AL} \qquad \text{at } X = L \tag{4}$$

$$C_A = 0 \qquad \text{at } t = 0 \text{ for } 0<X\leqslant L \tag{5}$$

where M is the strength of the input pulse, and V_3 and F are the volume of the lower chamber and the flow rate through it. Equation (4) is based on a uniform concentration C_L in the chamber equal to the outlet concentration and on negligible mass transfer resistance between pellet face and gas. These restrictions, requiring complete mixing in the lower chamber, can be approached closely by proper design of the apparatus. Furthermore, the pellet-chamber system can be designed and operated at conditions, for example F = 60 cm^3/min. and V_3 = 0.5 cm^3, such that the accumulation term $V_3\left(\frac{dC_{AL}}{dt}\right)$ in equation (4) is negligible.

Equations (1) to (5) can be solved in the Laplace domain with parameters for $C_A = f(x,s)$. Then using the relation

$$M_n = (-1)^n \lim_{S\to 0} \frac{d^n C_A}{dS^n} \tag{6}$$

gives a theoretical expression for the moments. The first normalized moment for the pellet is (12)

$$(\mu_1)\ \text{corr.} = \frac{M_1}{M_o} = \frac{L^2\varepsilon_p\left(3\frac{A}{L}De+F\right)}{6De\left(\frac{A}{L}De+F\right)} \tag{7}$$

Experimental values of the first moment can be determined from the observed response peaks using the equation

$$(\mu_1)\text{obs.} = \frac{\int_0^\infty C_A t\, dt}{\int_0^\infty C_A\, dt} \tag{8}$$

To obtain the moments for the pellet, the observed values should be corrected for the dead time in the volume between the injection point and the upper face, and between the lower face of the pellet and the detector, and for the injection time of the pulse, according to the equation

$$(\mu_1)\text{corr.} = (\mu_1)\text{obs.} - (\mu_1)\text{d.v.} - \frac{t_o}{2} \tag{9}$$

where (μ_1)d.v. is the first absolute moment value for dead volumes, t_o is the injection time of pulse. The values of (μ_1)corr. determined from equation (9) may then be used in equation (7) to determine the effective diffusivity.

Thies (38) developed a computer program applying the above theory (refer to Appendix C). The experimental results, i.e., the observed response peaks, are used in the computer program to measure the effective diffusivity in porous pellets.

B. The Conversion Behavior of the Calcium Oxide Sulfation Reaction

There are some features of CaO sulfation that were presented by Hartman and Coughlin (18) and Borgwardt (3). For example, the porosity of the reacting particles and the sulfation reaction rate decrease rapidly with increasing conversion. The reaction also affects the pore size distribution within the solid and the diffusional resistance in

the interior of the particles becomes limiting only after the conversion reaches the value of 20% or higher. At low temperature, 590° - 680°C, and very low SO_2 concentration, 0.5%, the overall rate is controlled by the chemical reaction taking place on the grains of calcium oxide. Thus, all of the factors, pellet structural changes, reaction temperature and concentration of gaseous reactant could affect the sulfation rate. From the stoichiometry of the reaction, $CaO + SO_2 + \frac{1}{2} O_2 \longrightarrow CaSO_4$, the relation between reactants and products is

$$(\frac{Xy_1}{M_{CO}}) M_{CS} + y_1(1-X) = y_2$$

where y_1 and y_2 are initial and final weights of the CaO pellet before and after reaction, X is conversion ratio, and M_{CO} and M_{CS} are the molecular weight of CaO and $CaSO_4$. After simplifying, the equation is used to estimate the conversion:

$$X = \frac{1 - y_2/y_1}{1 - M_{CS}/M_{CO}}$$

C. Porosity Measurement

In the CaO sulfation reaction, pore diffusion necessarily accompanies the chemical reaction, so that the solid matrix through which diffusion is taking place may undergo changes during the process. Therefore, porosity is an important parameter for understanding the rate limiting mechanism. In general, the electron microscope and mercury intrusion porosimetry are used to accurately measure pellet porosity, but by using the

dimensions and weight of pellet, one can theoretically calculate the porosity as follows:

$$\text{the volume of solid in the pellet} = \frac{\text{weight of pellet}}{\text{density of pure CaO}}$$

$$\text{the actual volume of pellet} = \text{the cross-sectional area of pellet} \times \text{the length of pellet}$$

$$\text{the porosity of pellet} = 1 - \frac{\text{the volume of solid in the pellet}}{\text{the actual volume of pellet}}$$

IV. EXPERIMENT APPARATUS AND PROCEDURES

A. Description of Equipment

The apparatus used in this study includes pellet making equipment, chemical reaction equipment, and diffusivity measurement equipment.

1. Pellet making equipment

The pelleting equipment consists of a Carver laboratory hydraulic press and two dies. The press has an operating pressure ranging from 0 to 24,000 psig with a pressure precision of about $\pm$ 200 psig. In this study, the cylindrical die has a 2.54 cm inside diameter. Since it is necessary that the pellet be held in the die and put into the diffusion cell for diffusion measurement, i.e., the pellet and die don't separate before finishing the diffusivity measurement including the reaction period, the material of the die is very important. The material must not react with the pellet at high temperature, it must not react with the gaseous reactant, especially highly corrosive gas SO_2. The weight change of the die will affect the accurate weight estimation for the pellets after reaction and would cause some error in calculating the pellet conversion. Stainless steel 304 was used for the die. Corrosion test results showed only 0.026% weight gain in pure SO_2 after 30 minutes at 600°C temperature. That weight change can be neglected in the present research.

2. Chemical reaction equipment

A quartz tube reactor, a tubular furnace, and three flowmeters comprise the reaction system. The quartz tube reactor is 5.08 cm I.D. and 60 cm long. The top outlet is connected to the waste gas treatment solution, and the bottom one is the inlet for the gaseous reactants. Tygon tubes connect to the supply tanks. Because the flow rate of the gas must be held steady during a run, the flowmeters are equipped with needle valves. The solid reactant pellet is supported in a carbon steel basket and located at the midpoint of the tube reactor. The Lindberg model 54341 electrically heated tubular furnace with a Lindberg type 2200 solid state controller capable of controlling the temperature to within $\pm$ 0.5°C is the main source of energy for CaO sulfation. The available temperature range is 200 - 1200°C, but the highest temperature used for this experiment is 600°C. An Ohaus type Dial-o-Gram balance was used to determine the weights of pellets before and after reaction.

3. Diffusivity measurement equipment

The main parts here are the Wicke-Kallenbach type diffusion cell, the thermal conductivity detector, the Fisher recorder, and flow metering and controlling equipment. The diffusion cell is shown in detail in Figure 2. There are two inlets and two outlets for gases to pass through both sides individually. The upper stream from inlet A (see Figure 2) is brought to the top of the pellet through a 0.3 cm I.D., 16 cm long tube, flared into a nozzle on the end to minimize the upper dead volume

and to create a rapid flow of gases across the upper face of the pellet. Similarly, the lower stream through inlet B is passed directly across the lower face in the volume V_3. The outlets E and F are connected to the manometer by tubing with restricting valves to maintain the pressure constant on both sides of the pellet. The upper stream flows from the outlet C to the soap flowmeter to measure the gas flow rate. The pulsed gas which has passed through the pellet with the carrier gas is directed into the thermalconductivity detector through outlet D. Threaded joints fix both parts of the pellet holder and the teflon o-rings to ensure a seal between the ring mold and the pellet holders.

The thermalconductivity detector consists of two columns; the gas to be analyzed is passed through one of these while a reference gas is passed through the other. Each column contains electrically heated filaments that have a temperature-dependent resistance. The filaments are wired as a bridge circuit such that the signal from the bridge depends on the difference between the thermal conductivity of the gas mixture being analyzed and the reference gas. The cell is machined from a steel block and is held in a controlled ($\pm$ 0.2°C) temperature bath.

The response peak from the detector was recorded using a Fisher Recordall series 5000 recorder. An attenuator was used to adjust the voltage to obtain a clear and reliable peak on the chart paper.

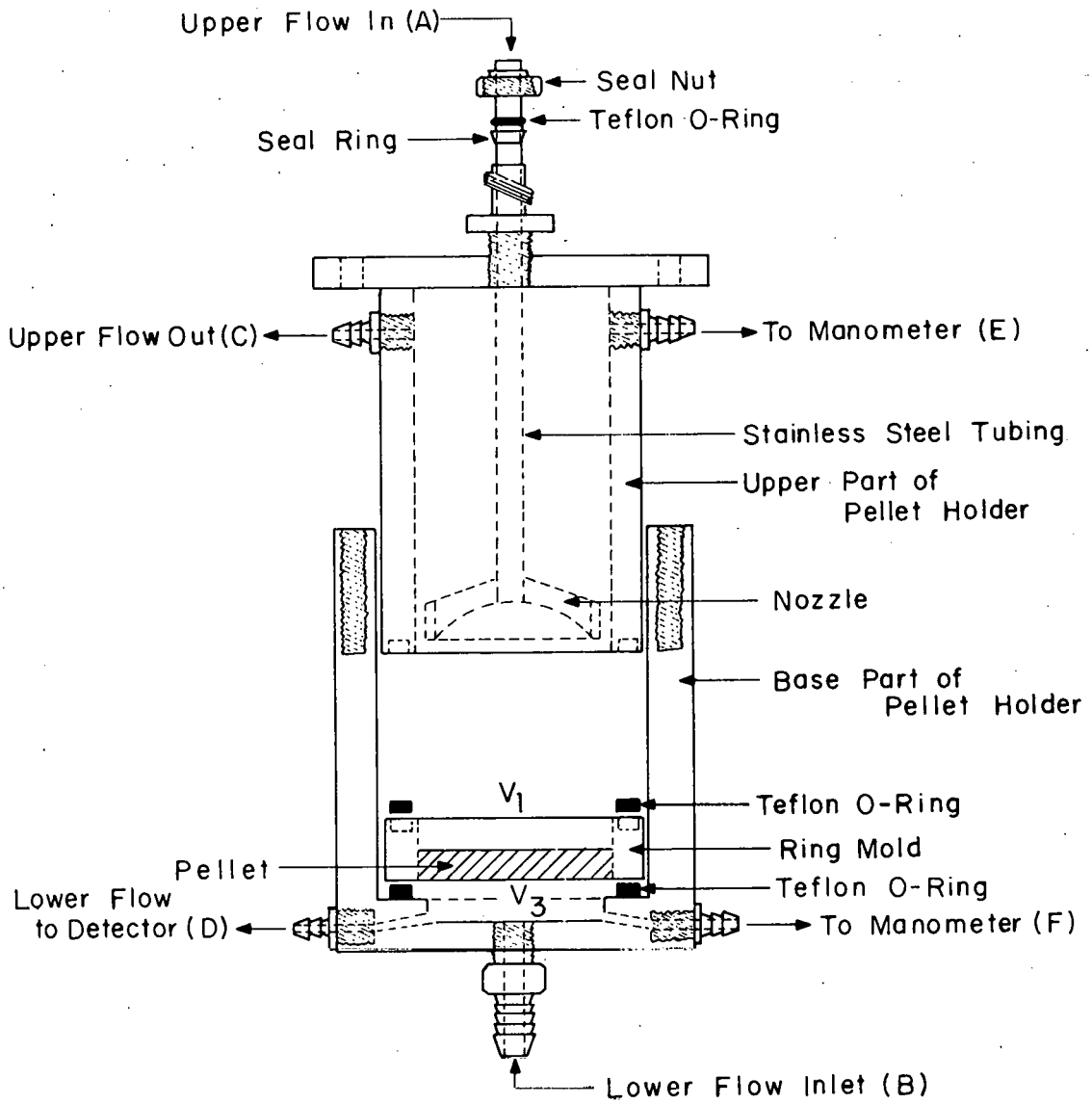

Figure 2. Schematic diagram of the Wicke-Kallenback type of diffusion cell

B. Experimental Procedure

The formation of the CaO pellet is an important step in the procedure. Homogeneous pellets without flaw are required to avoid experimental error. A new pellet, formed by the same procedure, was used in each conversion measurement experiment. Pellets with the same physical properties, i.e., pore size distribution, porosity, and surface area which affect the reaction rate directly, are needed. Calcium oxide absorbs moisture rapidly and becomes $Ca(OH)_2$ due to the reaction $CaO + H_2O \rightleftharpoons Ca(OH)_2$. Figure 3 shows the rate of moisture absorption. Pellets were therefore stored in a desiccator and handled in a dry box with minimal air contact to minimize the moisture absorption. The moisture weight of the CaO pellets was estimated conservatively as not over 0.5% pellet weight by using the electrobalance to measure weight change during the final drying step before reaction.

The CaO powder was prepared from Fisher Scientific Company's reagent grade 99.5% pure $Ca(OH)_2$. A quantity of $Ca(OH)_2$ was dehydrated, i.e., calcined, for 6 or 7 hours at 600°C in an oven to form CaO powder (5, 19). Pellets were formed by pressing the powder in a cylindrical mold of 2.54 cm diameter. Lengths of 0.24 to 0.30 cm were found to be the shortest pellets that would maintain their structural integrity.

Before putting the CaO pellet into the reactor to react and after finishing the reaction, the reactor system was purged with nitrogen for 10 to 20 minutes. The pellet was set at the center of tube reactor in a carbon-steel basket supported in the reactor. When the desired reaction temperature was reached, the metered and dried gaseous reactants,

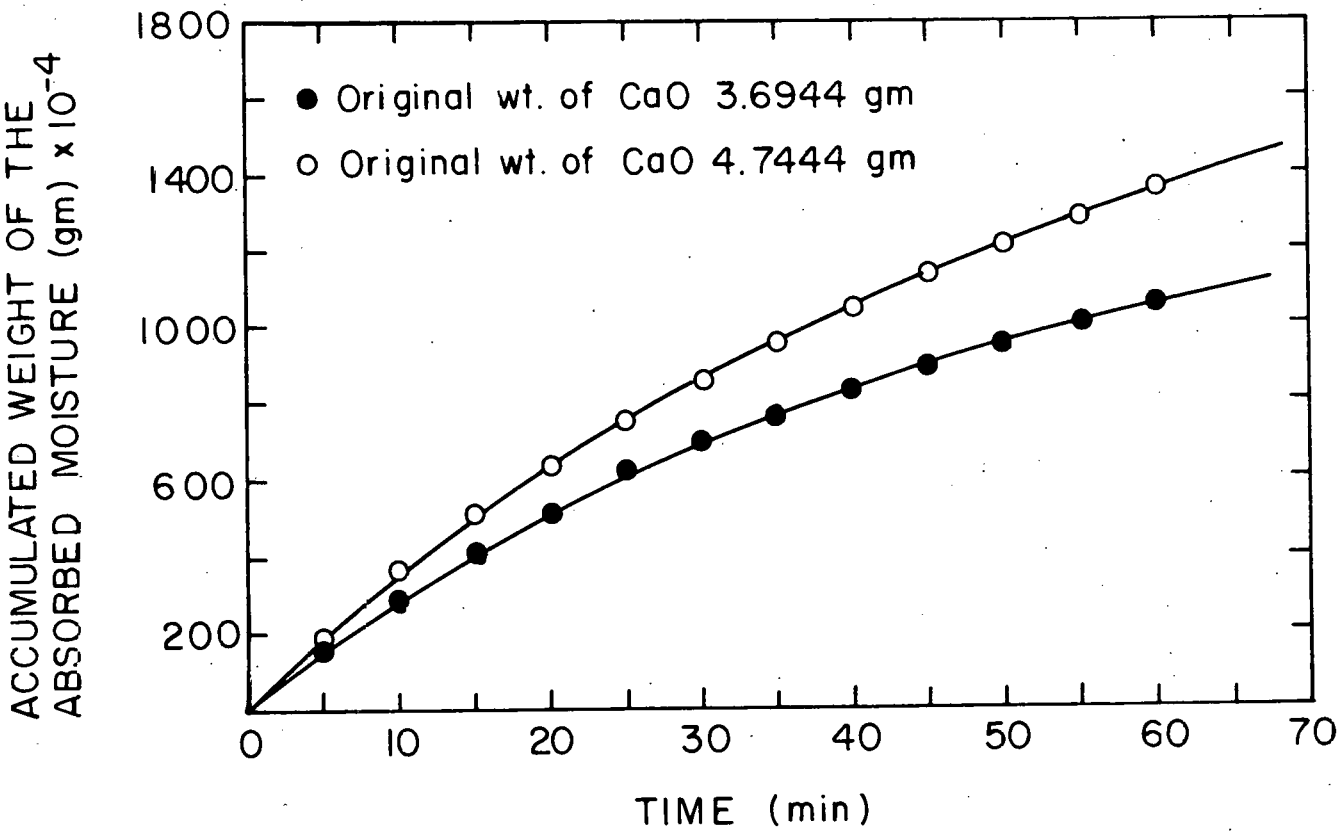

Figure 3. The rate of absorption on CaO

SO_2 540 cc/min and O_2 300 cc/min, were fed into the reactor from the bottom. By controlling the reaction time, a definite conversion could be obtained.

The procedure for measuring diffusivity is demonstrated using the flow chart in Figure 4. The diffusivity measuring system was purged for 10 to 15 minutes before sealing the CaO pellet in the diffusion cell. The metered nitrogen was then fed into the diffusion cell from two sides. The upper stream was brought to the top of the pellet through a 0.3 cm I.D., 16 cm long tube flared on the end. The lower stream was passed directly across the lower face. The pressure was maintained constant on both sides of the pellet, and the pressure difference was observed with the manometer. After obtaining equal pressures, the manometer was disconnected prior to injecting the He pulse to eliminate an additional contribution to the dead volume.

After obtaining equal pressures, a definite volume of helium which filled the tube between valves 2 and 3 was pulsed into the diffusion cell. The response peak was recorded from the thermal conductivity. Similarly, by switching the valves 1, 4, 5, and 6, a calibration response peak for a helium pulse which did not pass through the diffusion cell was obtained.

The measurements were made at 24°C and 1 atm. The data from the two recorded response peaks were divided into 64 values over equidistant time intervals of 0.48 sec. Pellet length, surface area of pellet, porosity, flow rate of carrier gas N_2(150 cc/min), and the initial guess values for dead time (2 sec.),

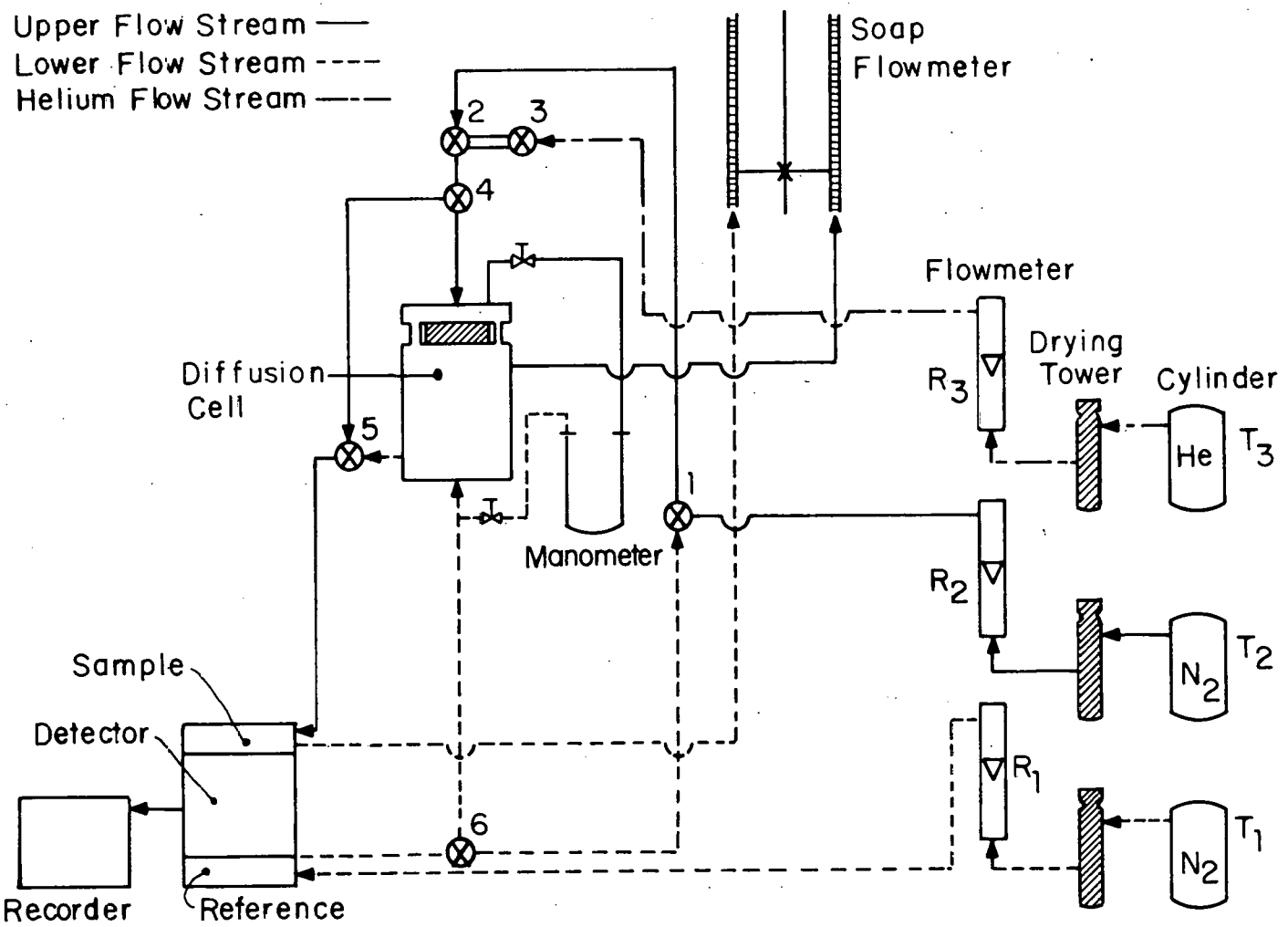

Figure 4. Schematic flow diagram for diffusivity measurement

diffusivity (0.1), residence time τ (0.8 sec.), and scale factor (the ratio of voltage strength of the two recorded response peaks) was used in the computer program (see Appendix C) to calculate the effective diffusivity.

V. RESULTS AND DISCUSSION

A. Preliminary Experiments for Diffusivity Measurement

Gas-solid reactions are very complicated, and several variables affect the rate of diffusion through a reacting solid pellet. In addition, the equipment available for diffusion measurement has inherent limitations on the precision of measured diffusivities, even if the pellet dimensions and porosity are held constant. The factors which affect experimental precision are, therefore, discussed first.

1. The effect of pellet length

Cylindrical pellets were made using different amounts of CaO in the same ring mold and pelletized under the same pressure. It was found that the pellet length was proportional to the weight of CaO. However, the diffusivity was inversely proportional to CaO weight, i.e., the diffusivity of the same diameter pellet decreases when the length of pellet increases. The experimental results are shown in Table 1. Besides, cylindrical pellets that have heights approaching or exceeding their diameters will exhibit nonuniform porosity because the compaction pressure is not uniform under these cases (37).

2. The effect of the height of nozzle in the diffusion cell

The distance between nozzle and the upper surface of the CaO pellet can be adjusted by shifting the stainless steel tubing which connects to the nozzle. Too large a distance causes too much upper dead volume, and

Table 1. The effect of CaO pellet length on diffusivity

Run	Length of pellets (cm)	Weight of pellets (gm)	Porosity (estimated)	Diffusivity (cm^2/sec)
1	0.20	1.500	0.5542	0.1095
2	0.25	1.935	0.5400	0.0907
3	0.39	2.975	0.5470	0.0843
4	0.43	2.800	0.6130	0.0716
5	0.42	3.190	0.5485	0.0533

too short a distance causes pressure diffusion. The appropriate height is necessary to avoid these effects. The results of measuring diffusivities with different nozzle height are shown in Table 2. The volume of the upper chamber was 0.45 cm^3 in Smith's investigation (32), and the nozzle height was estimated as about 0.3 cm from the geometry.

3. The relationship between reaction rate and reaction conditions

The conversion is hard to precisely control because of too many dependent factors as mentioned before. An attempt was made to get 20% conversion for each of several pellets made by identical procedures and using the same reaction conditions. Table 3 shows the results which suggest that more careful experimental operation and more precise equipment are needed. By using statistical methods on the experimental data

Table 2. The effect of the height of nozzle in the diffusion cell

Run	Length of pellets (cm)	Weight of pellets (gm)	Porosity (estimated)	Diffusivity (cm^2/sec)	Height of nozzle (cm)
1[a]	0.265	1.975	0.5570	0.1174	0.15
2	0.265	1.975	0.5570	0.1007	0.30
3	0.265	1.975	0.5570	0.0949	0.45
4	0.25	1.970	0.5316	0.0919	0.30
5	0.25	1.880	0.5530	0.0872	0.45

[a]The same pellet was used for runs 2 and 3.

in Table 3, the following results were obtained: porosity - mean value of 0.54, standard deviation 0.03, coefficient of variance 5.6%; conversion - mean value 19.0%, standard deviation 2.3, coefficient of variance 12.1%; diffusivity - mean value 0.046, standard deviation 0.008, coefficient of variance 16.8%.

The experimental results obtained, therefore, have sufficient precision for comparison of pellets with different conversions and porosities but the magnitude of the diffusivity is not of high precision.

Table 3. The results of 20% conversion experiments for CaO sulfation

Run	Length of pellet (cm)	Before reaction: Weight of pellet (gm)	Before reaction: Porosity (est.)	After reaction: Weight of pellet (gm)	After reaction: Conversion Ratio (%)	Diffusivity (cm^2/sec)
1[a]	0.25	1.930	0.5411	2.490	20.32	0.0435
2	0.26	1.930	0.5587	2.420	17.78	0.0648
3	0.26	1.900	0.5656	2.360	16.96	0.0455
4	0.26	1.945	0.5553	2.535	21.25	0.0421
5	0.26	1.975	0.5485	2.480	17.91	0.0468
6	0.26	1.945	0.5553	2.590	23.23	0.0462
7	0.255	1.910	0.5548	2.340	15.77	0.0492
8	0.26	1.975	0.5485	2.530	19.68	0.0360
9	0.26	1.940	0.5565	2.410	16.97	0.0419
10	0.21	1.910	0.4593	2.455	19.98	0.0406

[a]Reaction conditions: Temperature 400°C, reaction time 15 minutes, flow rate SO_2 540 cc/min, O_2 300 cc/min.

B. Diffusivities in Partially-reacted Calcium Oxide Pellets

There are two important points in connection with determination of diffusivities in porous media for gas-solid reaction studies: (a) for a binary gas mixture, it is frequently necessary to measure two or even three diffusivities, i.e., the Knudsen diffusivity, molecular diffusivity, and effective diffusivity, and (b) it is difficult to determine diffusivities within a reacting solid matrix, especially at high temperature. Few investigators of gas-solid reactions have carried out independent measurement of even a single gas diffusivity within the solid, and even fewer have done so at reaction conditions. Thus, the results presented here on diffusivity should aid in interpreting other results.

In this work, the pulse-response technique was used to measure the effective diffusivities, and appropriate models were used to calculate the Knudsen diffusivity and molar diffusivity. Although the effective diffusivities obtained by using N_2 and He in the diffusion cell are not true values of SO_2 and O_2 diffusion in the CaO sulfation reaction, the results illustrate the effect of structural changes of CaO pellets during the sulfation reaction. The results from the pulse-response technique can, therefore, be used to fit the gas-solid reaction models.

1. Conversion versus reaction time

The experiments of conversion versus reaction time were done at three different temperature levels, 325°C, 500°C and 600°C, for 20,000 psi compressed pellets by changing only the reaction time. The results

show that higher reaction temperature gives higher conversion for the same reaction time. The experimental results are recorded in Tables 4, 5, and 6 in Appendix B and in Figure 5. The lines drawn in Figure 5 simply identify the trends--they are not based on a model.

Different results have been reported at higher temperatures (over 650°C) by Christman (9), i.e., higher temperature gives lower conversion. Christman suggests that this is due to sintering and a lower gaseous reactant absorption rate. At low temperature that is not important. Because the melting points of CaO and $CaSO_4$ are 1257°C and 1450°C, the Tammann Temperature, the temperature at which a solid begins to sinter, is about 765 - 861.5°k (492 - 588.5°C). Thus, the sintering effects should be small in this study.

2. Diffusivity versus conversion

Because of the pore volume reduction caused by the expansion of the $CaSO_4$ product layer into the pellet void regions, the rate of gaseous reactant diffusion into the pellet reduces as conversion increases. The reaction will become diffusion-controlled at some level of CaO conversion for this reason. Similarly, the reduction in the diffusion rate of gaseous reactants will slow down the conversion rate and ultimately stop the reaction. Results illustrating this phenomenon are presented in Figure 6. The curve is the theoretical estimate of diffusivity using the Yake model for diffusion in an expanding solid.

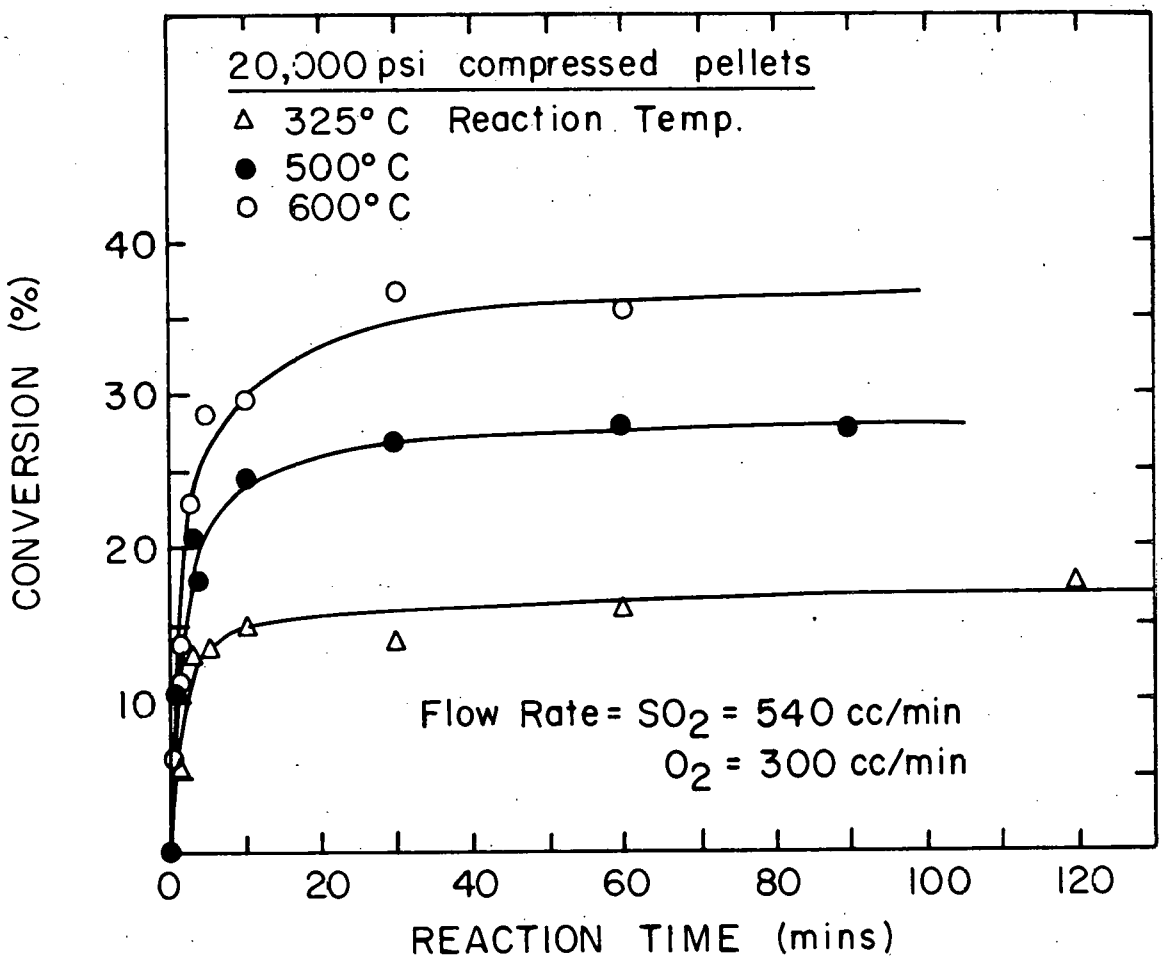

Figure 5. Effect of temperature on the conversion of CaO pellets

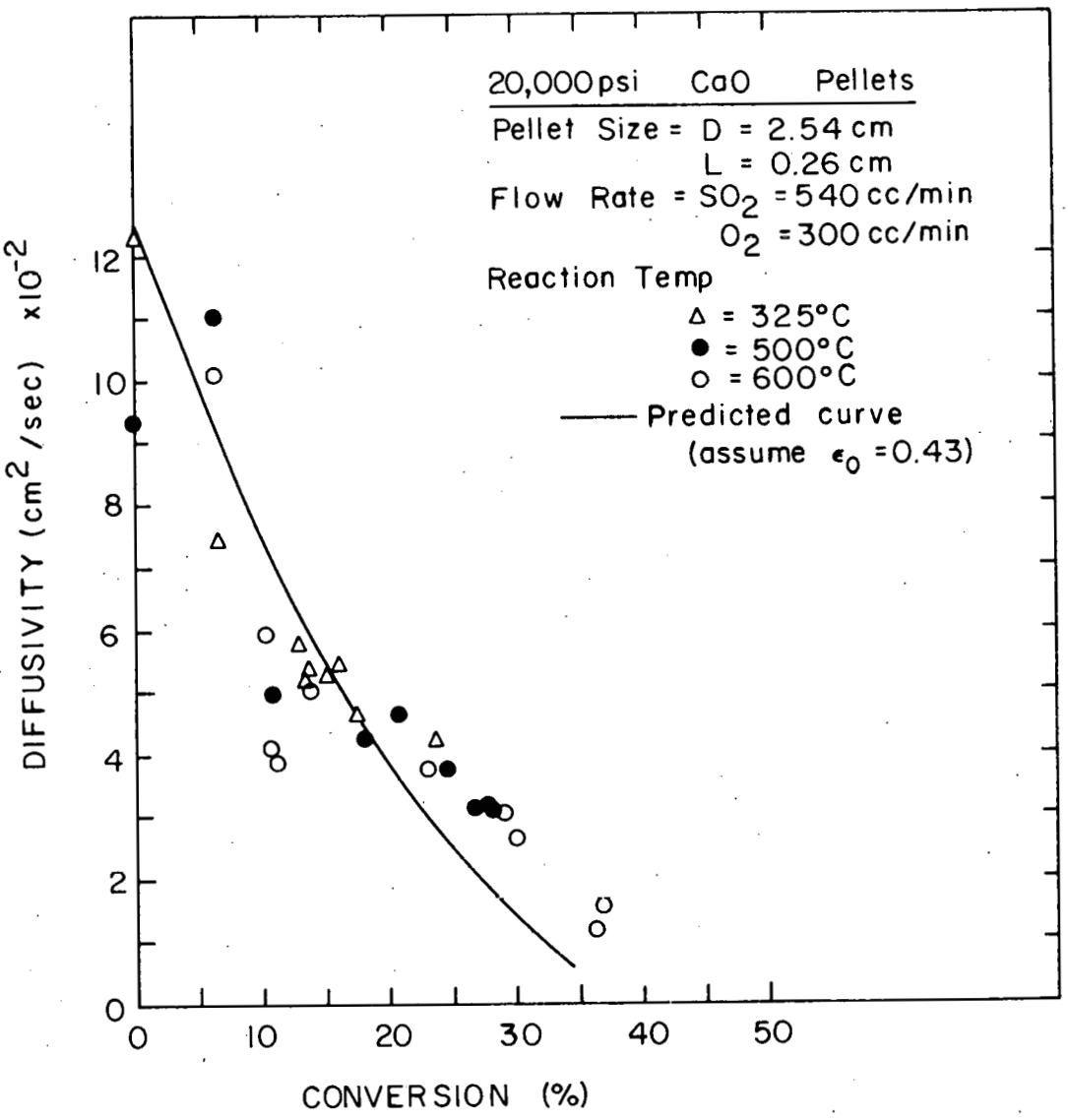

Figure 6. Diffusivity versus conversion in partially sulfated CaO pellets

According to the two-dimensional expanding grain model developed by Ulrichson and Yake (40), the initial effective diffusivity, D°_{EA}, is expressed in the following equation:

$$D^{\circ}_{EA} = \frac{1}{\frac{1}{D_{AC}} + \frac{\varepsilon_o^2}{D_{KA}}} \varepsilon_o^2$$

or, in general form, when porosity changes with conversion,

$$D_{EA} = \frac{1}{\frac{1}{D_{AC}} + \frac{\varepsilon^2}{D_{KA}}} \varepsilon^2 \qquad (10)$$

where D_{EA} is pellet effective diffusivity, ε is pellet porosity, D_{AC} and D_{KA} are molecular diffusivity and Knudsen diffusivity, respectively. The pellet porosity was assumed to have a linear relationship with conversion as shown in equation (11),

$$\varepsilon = \varepsilon_o - (1-\varepsilon_o)(\phi-1)X, \qquad (11)$$

where ϕ = expansion coefficient, 2.72 for CaO sulfation

X = conversion ratio.

The molecular diffusion D_{AC} can be calculated from the Chapman-Enskog kinetic theory (2, 37) using equation (12),

$$D_{AC} = 0.0018583 \frac{\sqrt{T^3(\frac{1}{M_A} + \frac{1}{M_C})}}{P\sigma_{AC}^2 \Omega_{D,AC}} \qquad (12)$$

The Knudsen diffusion, D_{KA}, is calculated from equations (13) and (14) (12),

$$D_{KA} = \frac{4}{3} \left(\frac{8RT}{\pi M_A}\right)^{\frac{1}{2}} K_o \tag{13}$$

$$K_o^{-1} = \frac{128}{9} \left(\frac{N_d \tau}{\varepsilon}\right) r_g^2 \left(1 + \frac{\pi}{8}\right), \quad \tau = \frac{1}{\varepsilon} \tag{14}$$

where σ_{AC} = collision diameter of species A and C, σ_{He,N_2} is 3.1285 Å

$\Omega_{D,AC}$ = dimensionless function of the temperature and of the intermolecular potential field for one mole of A and one of C, Ω_{D,HeN_2} is 0.7456

r_g = grain radius = $r_{go} [1 + (\phi-1)X]^{1/3}$,

r_{go} = initial grain radius = 3×10^{-4}cm (44),

N_d = no. of solid grains per unit volume of porous solid = $3(1-\varepsilon)/4\pi r_{go}^3$

R = gas constant = 8.314×10^7 gm.cm^2/°k sec^2.

At room temperature (25°C) and 1 atm pressure, the molecular diffusivity, D_{AC}, for helium and nitrogen is 0.70 cm^2/sec from equation (15). The Knudsen diffusivity has the following relation with conversion ratio and porosity for CaO sulfation,

$$D_{KA} = \frac{10.61(1 + 1.72X)\varepsilon^2}{(1-\varepsilon)(1 + 1.72X)^{2/3}}. \tag{15}$$

By using equations (10), (11) and (15) with the experimental conversion data, the estimated effective diffusivities for CaO sulfation can be compared to

the measured values. The estimated values for the different conditions are tabulated in Tables 10, 11, 12, 13 and 14 in Appendix B. From the calculated values, the Knudsen diffusivity is (3.45 cm^2/sec). The Knudsen term in equation (10) is about 4% of the molecular term, which suggests that the Knudsen diffusivity contributes little to the pellet effective diffusivity.

The agreement between the estimated values and the experimental results was good at low conversions, but the estimated diffusivities were low at higher conversions. Because porosity has a linear relation with conversion given by equation (11), the estimated porosity will become small at high conversion and the estimated diffusivity will also be small. But, a SEM examination of partially-reacted pellets revealed that the surface porosity, and hence the pellet porosity, did not become zero when reaction stopped. Consequently, the assumption of a linear variation in local porosity with conversion in equation (11) seems inappropriate. Yake (44) has pointed out that the minimum porosity concept can be used to correct for the deviation at high conversion. During CaO sulfation, as a result of a relatively large expansion coefficient, $\phi = 2.72$, continued reaction causes a significant drop in porosity that eventually restricts diffusion and results in a decrease of gaseous reactant concentration within the pellet. Therefore, the minimum porosity could be reached after which reaction continues at a finite rate, but the diffusivity no longer decreases. Obviously, the agreement between model and experiment will become better by applying the minimum porosity concept.

Although the sintering effect was assumed not to be important at low temperature, it could become important as the temperature approaches the

Tammann Temperature. In general, the agreement of estimated and experimental results looks better at low temperature (for example, 325°C in Table 10) than that at high temperature (for example, 500°C in Table 11). The deviation may have been caused by sintering because higher temperatures give a lower minimum porosity. At low temperature, the sintering effect is so small that a linear relationship between porosity and conversion ratio will be good. In contrast, it will be worse at higher temperature. Hence, if the minimum porosity concept and the sintering effect are considered, the agreement between the estimated values using the two-dimensional expanding grain model and experimental results could become better.

3. Diffusivity versus reaction time

The conversion of CaO pellets is proportional to reaction time before reaching the maximum conversion, but diffusivity is inversely proportional to conversion. Therefore, the diffusivity should be inversely proportional to reaction time, i.e., diffusivity decreases when reaction time increases as presented in Figure 7. The slopes of the diffusivity-reaction time curves become flat when reaction time is large, indicating that the porosity is no longer decreasing. Moreover, the higher the temperature, the lower the diffusivity for the same reaction time. This is due to higher conversion at higher temperature. Again, the estimated values from Yake's model have good agreement with experimental data at small reaction time but deviate at large reaction time, and the agreement at low temperature is better than at high temperature.

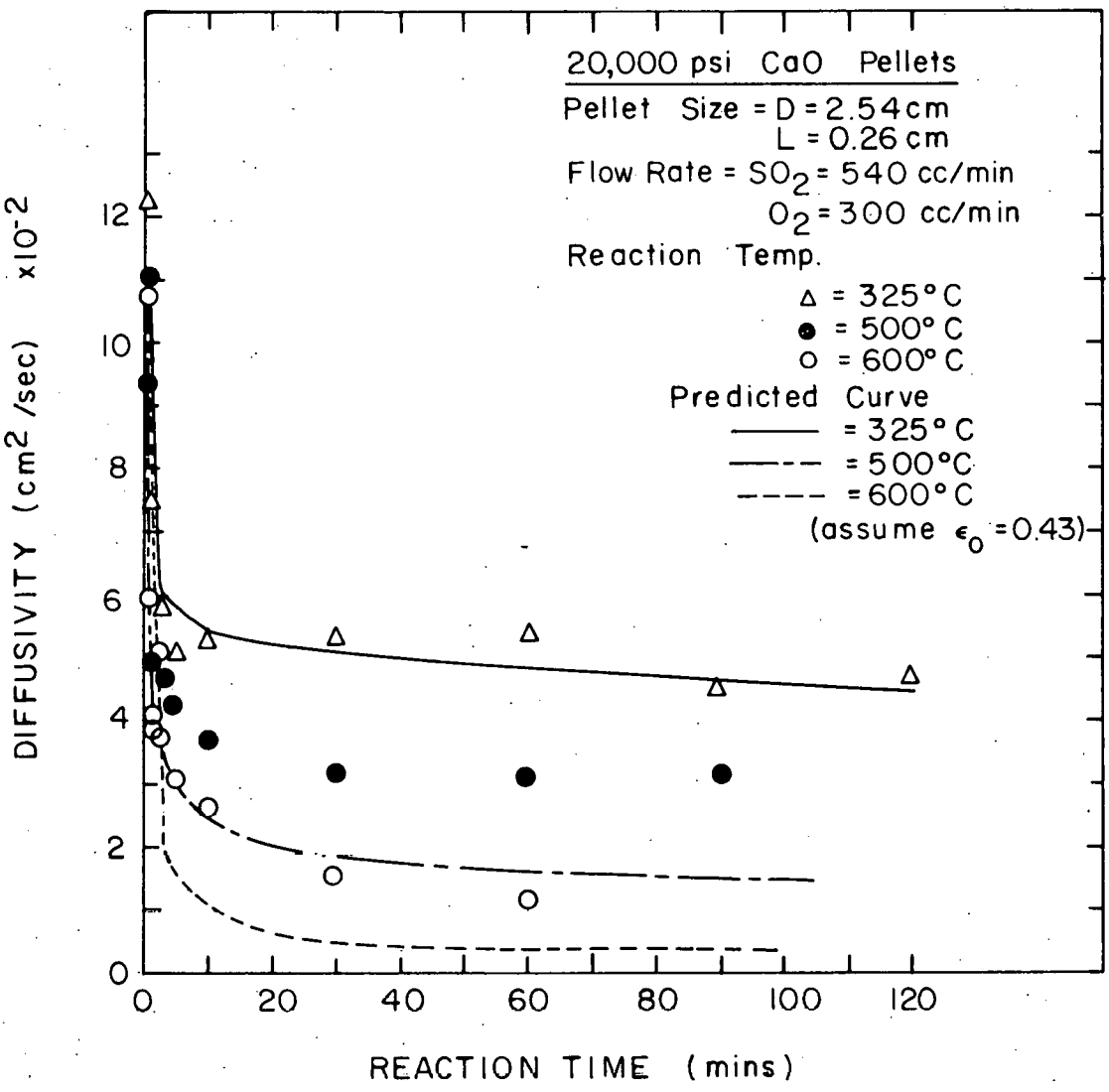

Figure 7. Diffusivity versus reaction time in partially sulfated CaO pellets

4. Conversion versus reaction time for different pelletizing pressures

Pellets formed by compressing to three different pressures, 10,000 psi, 20,000 psi, and 30,000 psi, were used. The corresponding estimated porosities were 0.47, 0.43, and 0.35. Because the mercury porosimeter has been out of order, just a few pellet porosities were measured. The porosimetry measured value for a 20,000 psi compressed pellet with 3.32% conversion was 0.4248, while the assumed initial value was 0.43. (The calculated initial value from Table 3 was 0.44.) These values compare well to the 0.39 value which Yake used for modeling. The estimated porosity differences are 0.04 between 30,000 psi and 20,000 psi, and 0.05 - 0.08 between 20,000 psi and 10,000 psi. So, the assumed values of 0.35 and 0.47 can be accepted.

The porosity of the pellets affected the reaction rate as expected in accordance with the work of others (3, 9). The more dense pellet has the lower reaction rate. The results can be used to infer that the reduction of porosity is the main reason for the reduced ultimate conversion. Experimental data are provided in Tables 5, 7, and 8 in Appendix B and in Figure 8. Again, the curves are only graphical estimates of the behavior.

5. Diffusivity versus conversion for different pelletizing pressures

For each pelletizing pressure, the diffusivity decreases as conversion increases and reaches a definite minimum value when the reaction stops. The more dense pellets have the lower diffusivity at a given conversion. The more dense pellets exhibit pore closure more rapidly and, therefore, the diffusivity decreases more rapidly. The results are

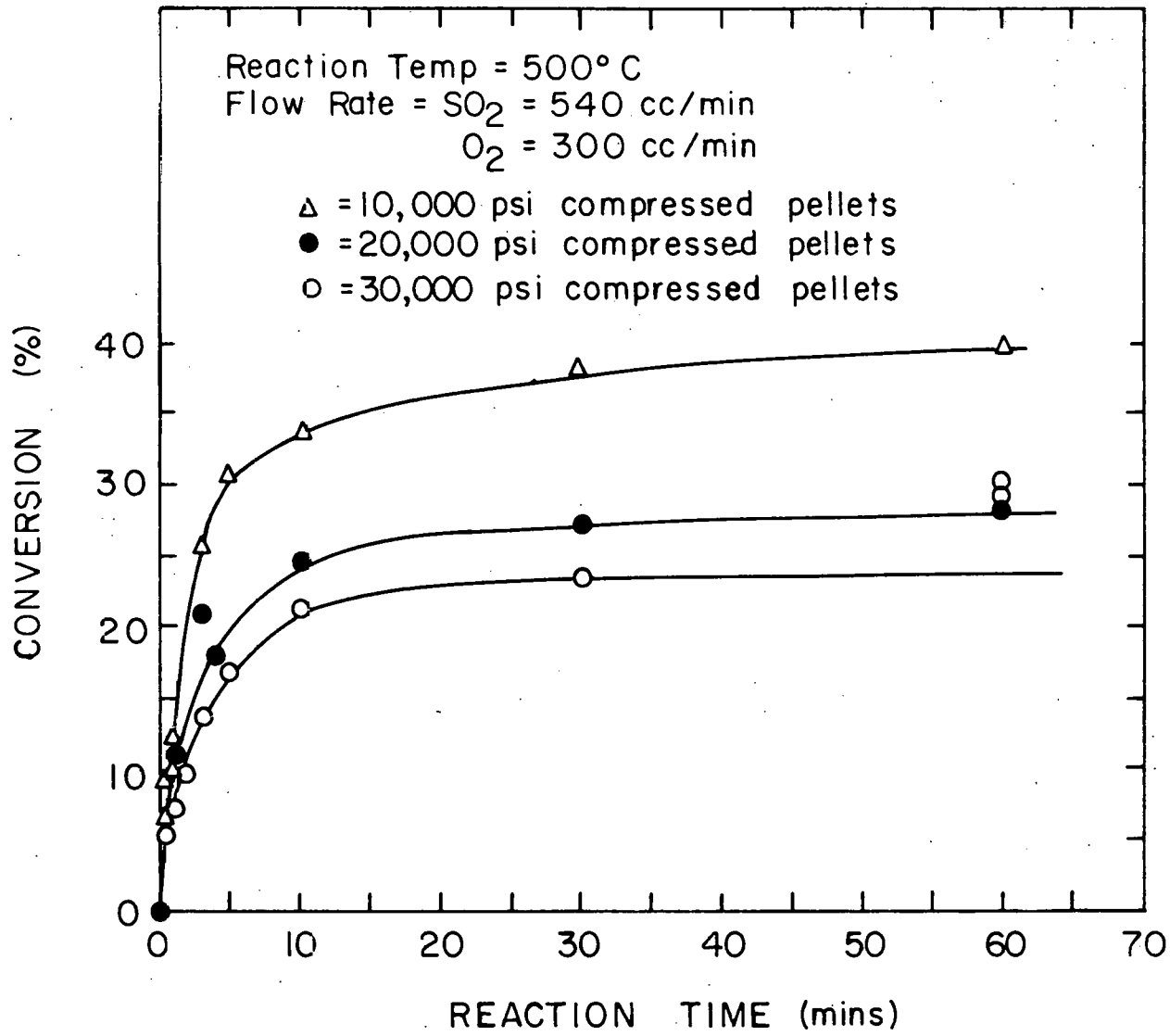

Figure 8. The relationship of conversion to reaction time for different pelletizing pressures

provided in Figure 9. The estimated values as shown by the curves were calculated from equations (10, (11), and (15).

6. Conversion versus reaction time for 20,000 psi compressed $Ca(OH)_2$ pellets

Experiments were also performed using $Ca(OH)_2$ powder as the raw material to form the pellets. The pellets were then calcined and sulfated at 600°C. The experimental results shown in Table 9 in Appendix B and Figure 10 compare well with those using CaO as the raw material. Both results should be the same if reaction conditions and pellet structure are kept the same.

7. Diffusivity versus conversion from 20,000 psi compressed $Ca(OH)_2$ pellets

In order to measure the diffusivity, the sulfated $Ca(OH)_2$ pellet in the ring mold must be set in the diffusion cell. That is, the ring mold contains the $Ca(OH)_2$ pellet during the calcination and sulfation operations. The diameter of the $Ca(OH)_2$ pellet reduces during calcination, and the pellet wants to drop out of the ring mold. This causes difficulty in the diffusivity measurement. The problem was solved by using grease to seal the gap between the sulfated pellet and the ring mold. Because the surface area of the sulfated $Ca(OH)_2$ pellet was smaller than that of the sulfated CaO pellet, the measured diffusivity for the former was a little smaller than that for the latter. But the

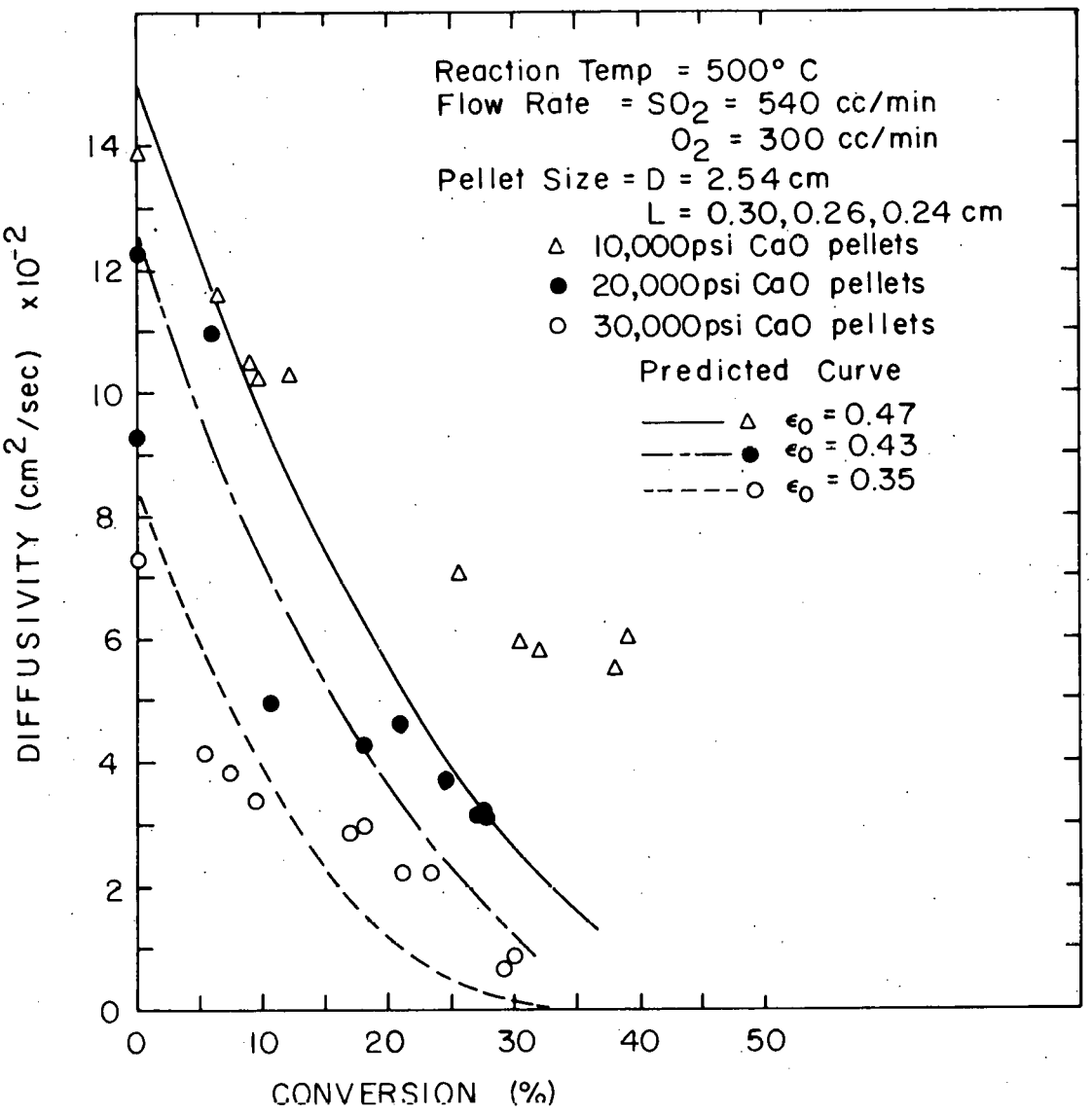

Figure 9. Diffusivity versus conversion for different pelletizing pressures

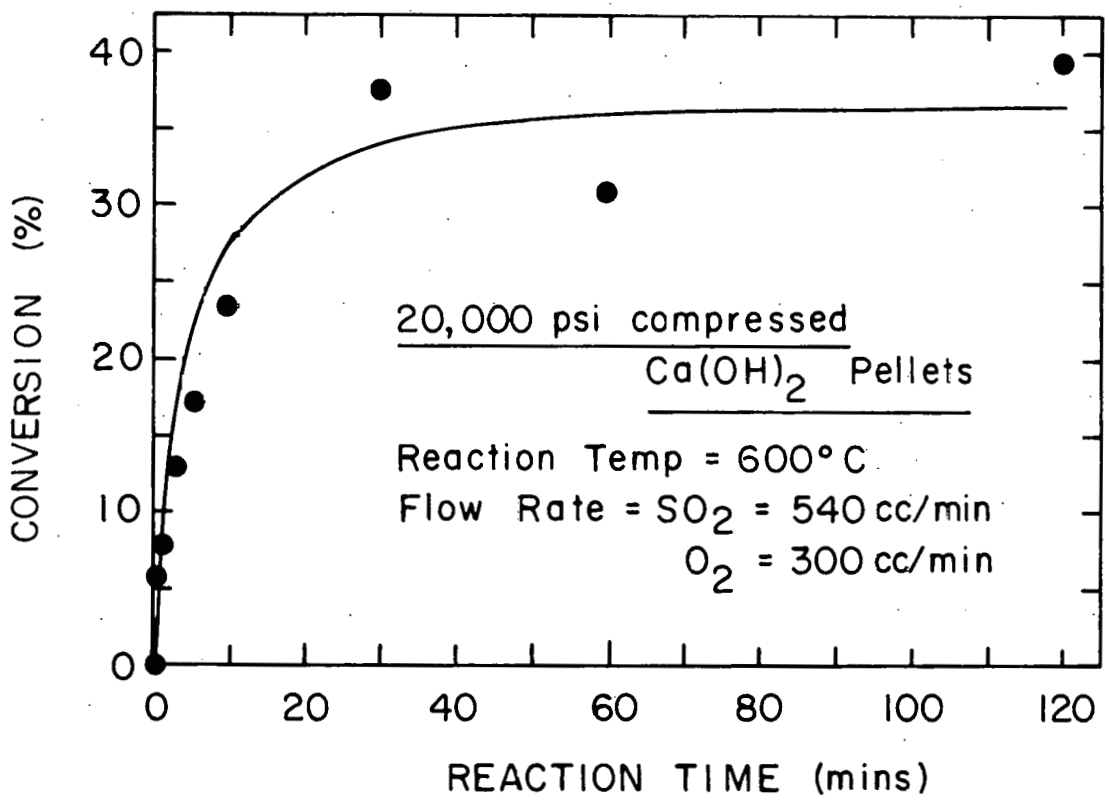

Figure 10. Conversion versus reaction time for 20,000 psi compressed $Ca(OH)_2$ pellets at 600°C

relationship of conversion ratio with respect to diffusivity was the same as the results in Figure 6. The experimental results are plotted in Figure 11. The curves in Figures 10 and 11 are only graphical estimates of the behavior, also.

8. Comparison of experimental results to those from C. Georgakis' model

C. Georgakis et al. (18) derived an equation to illustrate the porosity and conversion relation for limestone sulfation. For calcium oxide, we can simplify the equation to:

$$\varepsilon = 1 - (1-\varepsilon_o) \frac{\rho}{M_{CO}} [V_{CO} + X (V_{CS} - V_{CO})] \qquad (16)$$

where ε_o = initial porosity of CaO,

ρ = density of the unreacted crystalline solid CaO,

M_{CO} = molecular weight of CaO,

V_{CO} = molar volume of CaO,

V_{CS} = molar volume of $CaSO_4$,

X = conversion ratio.

Equation (16) was used to estimate the pellet porosity from experimental conversion data for the 20,000 psi compressed pellets at 325°C. The results are the same as those by using Yake's model.

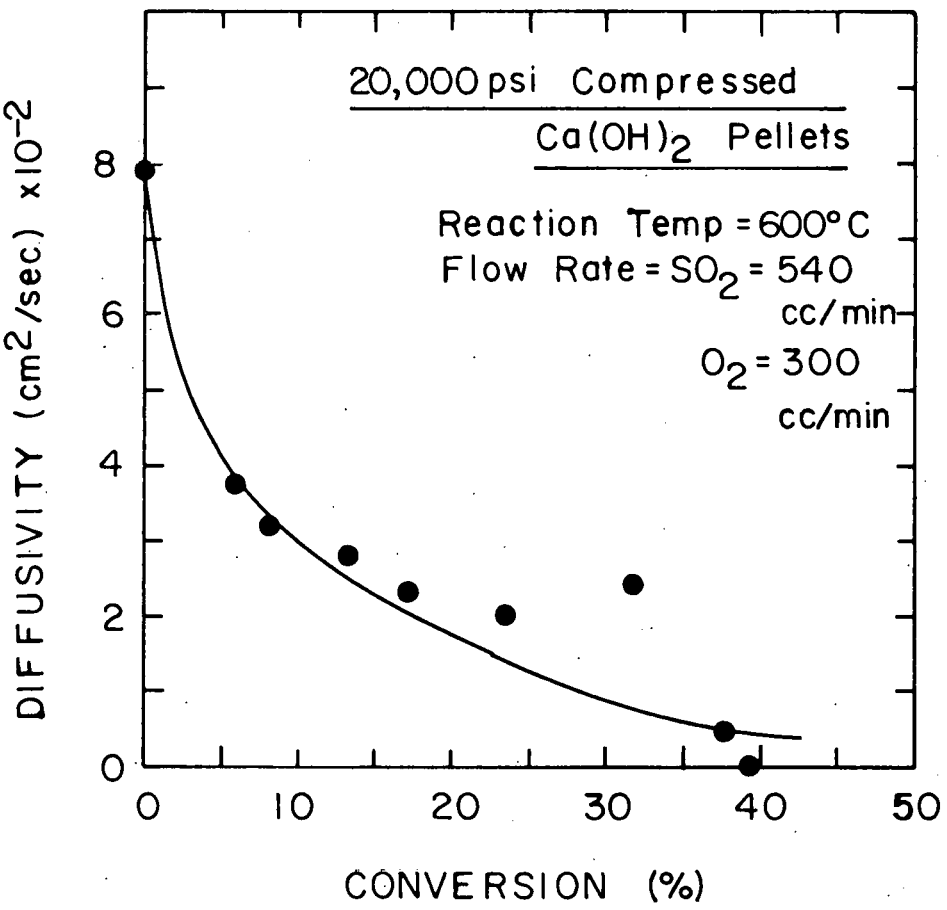

Figure 11. Diffusivity versus conversion for 20,000 psi compressed $Ca(OH)_2$ pellets at 600°C

9. Comparison of experimental results to those from Smith's model

Considering the effect of sintering, Ramachandran and Smith (23) presented a complicated model to demonstrate the relation of conversion to effective diffusivity. At 325°C, the sintering effect can be neglected in CaO sulfation so that the equations simplify to:

$$D_e = D[1 - (1-\varepsilon_o)(\frac{r_g}{r_{go}})^3]^2 \qquad (17)$$

and

$$r_g = r_{go}\,[1 + (\phi-1)X]^{1/3} \qquad (18)$$

where D is composite diffusivity accounting for Knudsen and bulk diffusion of species A,

$$D = \frac{1}{\frac{1}{D_{AC}} + \frac{\varepsilon^2}{D_{KA}}}$$

The estimated values using equations (17) and (18) are the same as those by using Yake's model.

VI. CONCLUSIONS

From the experimental measurement of diffusivity in CaO pellets during sulfation, it may be concluded that:

1. Because many factors affect experimental results, for example, moisture, pelletizing pressure, reactant flow rate, and nozzle height in diffusion cell, a careful and detailed operation was required in this experiment.
2. Experimental data showed that conversion increased as reaction time increased but became constant when it reached a certain level.
3. The reaction rate of CaO sulfation increases as temperature increases from 300 to 600°C.
4. During CaO sulfation, the diffusivity decreases as reaction time and conversion increase.
5. The reaction rate of the more dense CaO pellets during sulfation was lower than that of the less dense pellet, and the denser pellet had the lower diffusivity.
6. The change of conversion with time for a pellet was almost the same whether CaO or $Ca(OH)_2$ was used as the starting material. However, the diffusivity of the $Ca(OH)_2$ pellet was a little smaller than that of the CaO pellet because of a smaller surface area and grease contamination of the $Ca(OH)_2$ pellet.
7. The expanding grain model was used to fit the experimental results with agreement being better at low conversions than at high conversions. This was due to the linear relationship between porosity and

conversion in the model. If the minimum porosity concept and sintering effect were considered, the agreement would probably become better for high conversions.

VII. RECOMMENDATIONS FOR FUTURE RESEARCH

Experience gained through this investigation suggests several areas of research that should be explored and changes that should be made in the equipment for the diffusivity measurement in CaO pellets during sulfation. The recommendations are:

1. The $Ca(OH)_2$ powder was a product of Fisher Scientific Company with 99.5% pure $Ca(OH)_2$ and about 90% powder size between 200-400 mesh. The wide powder size range may cause enough variation of the pellet structure to be significant despite the very similar porosities of pellets. The original pellet structure variation would affect the precision of experimental conversion results, and this also affects the diffusivity. Therefore, careful screening of $Ca(OH)_2$ seems to be necessary.
2. The laboratory hydraulic press which we used to make pellets has a pressure range of 0 to 24,000 psig. Investigations at pressures higher than 24,000 psig would be desirable. Moreover, it is manually operated and would be hard to handle at definite pressure, especially near the maximum operating pressure (for example, 23,562 psig pressure was used for making the 30,000 psig compressed pellet with 1 inch diameter in this experiment). This would affect pellet porosity directly. Hence, a wider pressure range and easier handling press is needed.

3. Lacking a large enough electrobalance, it was difficult to achieve a specific conversion ratio in this research. It would be easier to control conversion if a big electrobalance was used with which pellet conversion could be monitored from the recorder as pellet weight changed.

VIII. BIBLIOGRAPHY

1. Bhatia, S. K., and Perlmutter, D. D. 1981. The effect of pore structure on fluid-solid reactions: Application to the SO_2-lime reaction. A. I. Ch. E. J. 27, no. 2:226.

2. Bird, R. B., Stewart, W. E., and Lightfoot, E. N. 1960. Transport Phenomena. New York: Wiley, 1960.

3. Borgwardt, R. H. 1970. Kinetics of the reaction of SO_2 with calcined limestone. Environ. Sci. Technol. 4:59.

4. Borgwardt, R. H., and Harvey, R. D. 1972. Properties of carbonate rocks related to SO_2 reactivity. Environ. Sci. Technol. 6:350.

5. Boynton, R. S. 1966. Chemistry and technology of lime and limestone. New York: Wiley.

6. Brown, L. F., Haynes, H. W., and Manogue, W. H. 1969. The prediction of diffusion rates in porous materials at different pressures. J. Catalysis 14:220.

7. Burghardt, A., and Smith, J. M. 1979. Dynamic response of a single catalyst pellet. Chem. Eng. Sci. 34:267.

8. Calvelo, E., and Smith, J. M. 1970. Intrapellet transport in gas-solid noncatalystic reactions. Chemica 1970:1.

9. Christman, P. G., and Edgar, T. F. 1980. The effect of temperature on the sulfation of limestone. 73rd annual meeting, A. I. Ch. E., Chicago.

10. Chrostowski, J. W., and Georgakis, C. 1978. A pore plugging model for gas-solid reactions. Paper presented at the 5th International Symposium on Chemical Reaction Engineering, Houston, Texas.

11. Dogu, Gulsen. 1974. Intrapellet rate parameters by single pellet chromatography. Ph.D. dissertation, University of California, Davis.

12. Dogu, Gulsen, and Smith, J. M. 1975. A dynamic method for catalyst diffusivities. A. I. Ch. E. J. 21, no. 1:58.

13. Dogu, Gulsen, and Smith, J. M. 1976. Rate parameters from dynamic experiments with single catalyst pellets. Chem. Eng. Sci. 31:123.

14. Evans, R. B., Watson, G. M., and Mason, E. A. 1961. Gaseous diffusion in porous media at uniform pressure. J. Chem. Phys. 33:2076.

15. Georgakis, C., et al. 1977. Modeling desulfurization reactions in fluidized bed combustors. 5th International Conference on Fluidized Bed Combustion, Washington, D.C.

16. Gokarn, A. N., and Doraiswamy, L. K. 1972. Measurement of diffusion in the ash layer in gas-solid reactions. Chem. Eng. Sci. 27:1515.

17. Hartman, M., and Coughlin, R. W. 1974. Reaction of sulfur dioxide with limestone and the influence of pore structure. Ind. Eng. Chem. Proc. Des. Dev. 13:248.

18. Hartman, M., and Coughlin, R. W. 1976. Reaction of sulfur dioxide with limestone and the grain model. A. I. Ch. E. J. 22, no. 3:490.

19. Hursh, R. K., and Clemens, E. C. 1931. Effects of body composition and firing treatment on salt glazes. Trans. Am. Ceram. Soc. 14:482.

20. Johnson, M. F. L., and Stewart, W. E. 1965. Pore structure and gaseous diffusion in solid catalysts. J. Catalysis 4:248.

21. Kim, K. K., and Smith, J. M. 1974. Diffusion in nickel oxide pellets: Effects of sintering and reduction. A. I. Ch. E. J. 20, no. 4:670.

22. Marsh, D. Kinetics of calcium oxide sulfation and pore closure models. Private communication, Chem. E. Dept., Iowa State Univ., Ames, Iowa.

23. Ramachandran, P. A., and Smith, J. M. 1977. Effect of sintering and porosity changes on rates of gas-solid reactions. Chem. Eng. J. 14:137.

24. Ramachandran, P. A., and Smith, J. M. 1977. A single-pore model for gas-solid noncatalytic reactions. A. I. Ch. E. J. 23, no. 3:353.

25. Ran, Abed, and Robert, G. R. 1973. Reaction with mole changes in porous catalysts in the molecular, transition, and Knudsen regimes. A. I. Ch. E. J. 19, no. 3:618.

26. Rao, M. R., and Smith, J. M. 1963. Diffusion resistances in alumina and silica catalysts. A. I. Ch. E. J. 9:419.

27. Rinker, R. G., and Chen, O. T. 1979. Modification of the dusty-gas equation to predict mass transfer in general porous media. Chem. Eng. Sci. 34:51.

28. Rothfeld, L. B. 1963. Gaseous counter diffusion in catalyst pellets. A. I. Ch. E. J. 9:19.

29. Satterfield, C. N. 1970. Mass transfer in heterogeneous catalysis. Cambridge, Mass.: MIT Press.

30. Satterfield, C. N., and Cadle, P. J. 1968. Diffusion in commercially manufactured pelleted catalysts. Ind. Eng. Chem. Proc. Des. Dev. 7:256.

31. Satterfield, C. N., Ma, Y. H., and Sherwood, T. K. 1968. The effectiveness factor in a liquid-filled porous catalyst. Chem. Eng. Symp. Ser. No. 28:22.

32. Smith, J. M. 1975. Chemical engineering kinetics. 2nd ed. New York: McGraw-Hill Co., 1975.

33. Sohn, H. Y., and Szekely, J. 1972. A general dimensionless representation of the irreversible reaction between a porous solid and a reactant gas. Chem. Eng. Sci. 27:763.

34. Suzuki, M., and Smith, J. M. 1972. Dynamic of diffusion and adsorption in a single catalyst pellet. A. I. Ch. E. J. 18:326.

35. Szekely, J. 1976. Paper presented at the 4th International Chemical Reaction Symposium, Heidelberg, W. Germany.

36. Szekely, J., and Evans, J. W. 1971. A structural model for gas-solid reactions with a moving boundary. Chem. Eng. Sci. 25:1091.

37. Szekely, J., Evans, J. W., and Sohn, H. Y. 1976. Gas-solid reaction. New York: Academic Press Co.

38. Thies, B. Diffusion measurement in calcium oxide pellet. Private communication, Chem. E. Dept., Iowa State Univ., Ames, Iowa.

39. Trimm, D. L., and Corrie, J. 1972. The effect of temperature on the diffusion of gases in oxide catalysts. Chem. Eng. J. 4, no. 3:229.

40. Ulrichson, D. L., and Yake, D. E. 1980. Numerical analysis of a finite cylindrical pellet model in solid-gas reactions. Chem. Eng. Sci. 35:2207.

41. Van Deemter, Zuiderweg, J. J., and Klinkenberg, A. 1956. Longitudinal diffusion and resistance to mass transfer as causes of nonideality in chromatography. Chem. Eng. Sci. 5:271.

42. Wakao, N., and Smith, J. M. 1962. Diffusion in catalyst pellets. Chem. Eng. Sci. 17:825.

43. Wicke, E., and Kallenbach, R. 1941. The diffusion bridge for porous solids. Kolloid, 2.97:135.

44. Yake, D. E. 1980. Modeling of bulk flow: Reversibility and pore closure with a grain model for gas-solid reactions. Kinetics of calcium oxide chlorination and pore closure models. Ph.D. thesis. Ames, Iowa, Library, Iowa State University of Science and Technology.

IX. ACKNOWLEDGMENTS

The author would like to express his appreciation to Dr. D. L. Ulrichson for suggesting this project and for the guidance he offered throughout the investigation.

Appreciation is also expressed to Dr. A. H. Pulsifer and Dr. Orville Hunter, Jr., for the many times they provided assistance throughout the research.

The author would like to especially express his appreciation to groupmates Dan Marsh and Bob Thies for the help they provided in discussing problems and assisting with the instrumentation for this investigation.

And, finally, the author expresses his appreciation to his wife, parents and friends for their patience and encouragement throughout the investigation.

X. APPENDIX A:

DERIVATION OF DIFFUSION EQUATION FOR DIFFUSIVITY MEASUREMENT USING DIFFUSION CELL

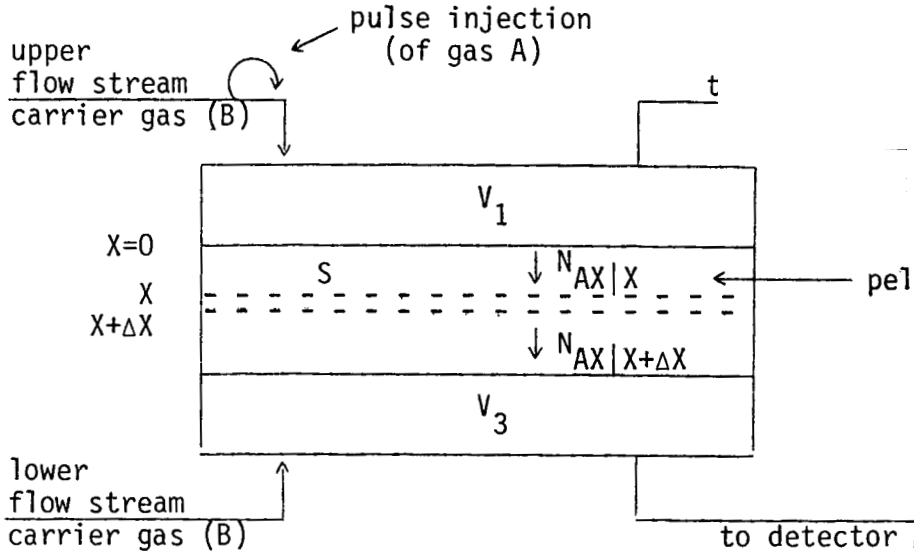

Mass balance for A

Input - Output = Accumulation

$$\therefore \quad N_{AX|X} \cdot S - N_{AX|_{X+\Delta X}} \cdot S = \frac{\partial C_A}{\partial t} \cdot S \cdot \Delta X \cdot \varepsilon_p$$

where S is cross-section area, ε_p is porosity of the pellet.

$$\therefore \quad - \frac{\partial N_{AX}}{\partial X} = \varepsilon_p \cdot \frac{\partial C_A}{\partial t}$$

For binary system

$$N_{AX} = -C\, D_{AB} \frac{\partial X_A}{\partial X} + X_A\, (N_{AX} + N_{BX})$$

where X_A is very small compared to X_B

The total concentration C can be assumed constant.

We used D_e instead of D_{AB} here, and D_e is constant because of independence of concentration (32).

$$N_{AX} = - D_e \frac{\partial C_A}{\partial X} \qquad (20)$$

Substitute equation (20) into (19),

$$D_e \frac{\partial^2 C_A}{\partial X^2} = \varepsilon p \cdot \frac{\partial C_A}{\partial t} \quad .$$

XI. APPENDIX B:

EXPERIMENTAL RESULTS

Table 4. The experimental data of sulfation reaction for 20,000 psi compressed CaO pellets at 325°C

			Before reaction		After reaction		
Run	Reaction time (min)	Lg. of pellet (cm)	Wt. of pellet (gm)	Porosity (est.)	Wt. of pellet (gm)	Conversion ratio (%)	Diffusivity (cm^2/sec)
1	0	0.255	1.990	0.5361	1.990	0	0.9320
2	0	0.285	1.975	0.5881	1.975	0	0.0891
3	1	0.260	2.010	0.5405	2.160	5.23	--
4	1	0.260	1.965	0.5507	2.145	6.42	0.0743
5	2.5	0.270	1.970	0.5663	2.335	12.98	0.0578
6	5	0.255	1.990	0.5361	2.370	13.38	0.0509
7	10	0.285	1.975	0.5881	2.395	14.90	0.0528
8	30	0.260	1.980	0.5473	2.365	13.62	0.0531
9	60	0.275	1.980	0.5720	2.430	15.92	0.0544
10	90	0.260	1.940	0.5565	2.595	23.65	0.0423
11	120	0.255	1.900	0.5571	2.375	17.51	0.0463

Table 5. The experimental data of sulfation reaction for 20,000 psi compressed CaO pellets at 500°C

Run	Reaction time (min.)	Lg. of pellet (cm)	Before reaction		After reaction		
			Wt. of pellet (gm)	Porosity (est.)	Wt. of pellet (gm)	Conversion ratio (%)	Diffusivity (cm^2/sec)
1	0.5	0.245	1.940	0.5293	2.110	6.12	0.1103
2	1	0.250	1.915	0.5447	2.205	10.61	0.0496
3	3	0.260	1.920	0.5610	2.490	20.80	0.0468
4	4	0.260	1.975	0.5485	2.480	17.91	0.0426
5	10	0.270	2.015	0.5564	2.720	24.51	0.0376
6	30	0.260	1.980	0.5473	2.740	26.89	0.0318
7	60	0.270	2.020	0.5553	2.830	28.09	0.0314
8	90	0.260	1.920	0.5610	2.685	27.91	0.0318

Table 6. The experimental data of sulfation reaction for 20,000 psi compressed CaO pellets at 600°C

Run	Reaction time (min.)	Lg. of pellet (cm)	Before reaction: Wt. of pellet (gm)	Before reaction: Porosity (est.)	After reaction: Wt. of pellet (gm)	After reaction: Conversion ratio (%)	After reaction: Diffusivity (cm^2/sec)
1	0.5	0.255	1.955	0.5443	2.130	6.27	0.1078
2	1	0.270	1.915	0.5784	2.195	10.24	0.0594
3	1.5	0.255	1.935	0.5489	2.245	11.22	--
4	1.5	0.260	1.960	0.5519	2.270	11.08	0.0389
5	1.5	0.260	1.990	0.5450	2.290	10.56	0.0409
6	2	0.265	1.880	0.5783	2.245	13.60	0.0501
7	3	0.270	2.000	0.5597	2.655	22.94	0.0377
8	5	0.280	1.955	0.5850	2.755	28.66	0.0307
9	10	0.270	1.975	0.5652	2.820	29.97	0.0265
10	30	0.270	1.995	0.5608	3.045	36.87	0.0153
11	60	0.260	1.960	0.5473	3.000	36.09	0.0119

Table 7. The experimental data of sulfation reaction for 10,000 psi compressed CaO pellets at 500°C

Run	Reaction time (min.)	Lg. of pellet (cm)	Before reaction: Wt. of pellet (gm)	Before reaction: Porosity (est.)	After reaction: Wt. of pellet (gm)	After reaction: Conversion ratio (%)	After reaction: Diffusivity (cm^2/sec)
1	0	0.275	1.910	0.5871	1.910	0	0.1389
2	0.33	0.300	2.020	0.5997	2.205	6.42	0.1160
3	0.5	0.300	1.955	0.6126	2.205	8.96	0.1047
4	0.67	0.295	2.015	0.5940	2.290	9.56	0.1021
5	1	0.310	1.995	0.6175	2.340	12.11	0.1032
6	3	0.290	1.935	0.6034	2.645	25.70	0.0706
7	5	0.300	1.990	0.6057	2.860	30.62	0.0597
8	10	0.300	1.950	0.6136	2.885	33.59	--
9	10	0.290	1.990	0.5921	2.900	32.03	0.0587
10	30	0.300	2.015	0.6007	3.110	38.07	0.0552
11	60	0.300	1.970	0.6097	3.070	39.11	0.0603

Table 8. The experimental data of sulfation reaction for 30,000 psi compressed CaO pellets at 500°C

			Before reaction		After reaction		
Run	Reaction time (min.)	Lg. of pellet (cm)	Wt. of pellet (gm)	Porosity (est.)	Wt. of pellet (gm)	Conversion ratio (%)	Diffusivity (cm^2/sec)
1	0	0.240	1.940	0.5195	1.940	0	0.0731
2	0.5	0.245	1.975	0.5208	2.130	5.50	0.0416
3	1	0.245	1.960	0.5245	2.165	7.33	0.0384
4	2	0.235	1.975	0.5004	2.245	9.58	0.0342
5	3	0.240	1.940	0.5195	2.320	13.72	--
6	3	0.245	1.935	0.5305	2.425	17.74	0.0295
7	5	0.255	1.940	0.5478	2.410	16.97	0.0287
8	10	0.250	1.975	0.5304	2.570	21.10	0.0221
9	30	0.235	2.000	0.4941	2.670	23.47	0.0226
10	60	0.245	1.925	0.5208	2.730	29.29	0.0065
11	60	0.240	1.885	0.5331	2.695	30.10	0.0089

Table 9. The experimental data of sulfation reaction for 20,000 psi compressed $Ca(OH)_2$ pellets at 600°C

Run	Reaction time (min.)	Lg. of pellet (cm)	Before reaction: Wt. of pellet $Ca(OH)_2$ (gm)	Before reaction: Wt. of calcined $Ca(OH)_2$ (gm)	After reaction: Wt. of pellet (gm)	After reaction: Conversion ratio (%)	After reaction: Porosity (est.)	After reaction: Diffusivity (cm^2/sec)
1	0	0.30	2.605	1.965	1.965	0	0.5487	0.0794
2	0.5	0.30	2.600	1.968	2.125	5.83	0.5491	0.0375
3	1	0.30	2.575	1.949	2.160	7.90	0.5524	0.0320
4	3	0.31	2.595	1.964	2.315	13.05	0.5611	0.0283
5	5	0.31	2.600	1.968	2.430	17.14	0.5603	0.0234
6	10	0.32	2.595	1.964	2.600	23.64	0.5717	0.0201
7	30	0.32	2.575	1.949	2.955	37.69	0.5742	0.0045
8	60	0.31	2.610	1.950	2.835	31.79	0.5587	0.0246
9	120	0.32	2.610	1.975	3.040	39.37	0.5698	0

Table 10. Comparison of estimated to experimental results for D. E. Yake's model at 325°C and 20,000 psi compressed pellets

Run	Reaction time (min.)	Conversion ratio (%)	Calc. porosity (assume ε_o=0.43)	Calc. diffusivity from calc. porosity (cm^2/sec)	Experimental diffusivity (cm^2/sec)
1	0	0	0.4300	0.1247	0.1228
2	1	6.42	0.3671	0.0906	0.0743
3	2.5	12.98	0.3027	0.0615	0.0578
4	5	13.38	0.2988	0.0599	0.0509
5	10	14.90	0.2839	0.0540	0.0528
6	30	13.62	0.2965	0.0590	0.0531
7	60	15.92	0.2739	0.0503	0.0544
8	90	23.65	0.1981	0.0262	0.0423
9	120	17.51	0.2583	0.0447	0.0463

Table 11. Comparison of estimated to experimental results for D. E. Yake's model at 500°C and 20,000 psi compressed pellets

Run	Reaction time (min.)	Conversion ratio (%)	Calc. porosity (assume ε_o=0.43)	Calc. diffusivity from calc. porosity (cm^2/sec)	Experimental diffusivity (cm^2/sec)
1	0	0	0.4300	0.1247	0.1228
2	0.5	6.12	0.3700	0.0921	0.1103
3	1	10.61	0.3260	0.0704	0.0496
4	3	20.80	0.2260	0.0342	0.0468
5	4	17.91	0.2544	0.0433	0.0426
6	10	24.51	0.1897	0.0240	0.0376
7	30	26.89	0.1664	0.0185	0.0318
8	60	28.09	0.1546	0.0159	0.0314
9	90	27.91	0.1564	0.0163	0.0318

Table 12. Comparison of estimated to experimental results for D. E. Yake's model at 600°C and 20,000 psi compressed pellets

Run	Reaction time (min.)	Conversion ratio (%)	Calc. porosity (assume ε_o=0.43)	Calc. diffusivity from calc. porosity (cm^2/sec)	Experimental diffusivity (cm^2/sec)
1	0	0	0.4300	0.1247	0.1228
2	0.5	6.27	0.3685	0.0914	0.1078
3	1	10.24	0.3296	0.0730	0.0594
4	1.5	10.56	0.3265	0.0716	0.0409
5	1.5	11.08	0.3214	0.0694	0.0389
6	2	13.60	0.2967	0.0591	0.0501
7	3	22.94	0.2051	0.0281	0.0377
8	5	28.66	0.1490	0.0148	0.0307
9	10	29.97	0.1362	0.0124	0.0265
10	30	36.87	0.0685	0.0031	0.0119
11	60	36.09	0.0762	0.0039	0.0153

Table 13. Comparison of estimated to experimental results for D. E. Yake's model at 500°C and 10,000 psi compressed pellets

Run	Reaction time (min.)	Conversion ratio (%)	Calc. porosity (assume ε_o=0.47)	Calc. diffusivity from calc. porosity (cm^2/sec)	Experimental diffusivity (cm^2/sec)
1	0	0	0.4700	0.1494	0.1389
2	0.33	6.42	0.4115	0.1142	0.1160
3	0.5	8.96	0.3883	0.1016	0.1047
4	0.67	9.56	0.3829	0.0988	0.1021
5	1	12.11	0.3596	0.0870	0.1032
6	3	25.70	0.2357	0.0372	0.0706
7	5	30.62	0.1909	0.0244	0.0597
8	10	32.03	0.1780	0.0212	0.0587
9	10	33.59	0.1638	0.0179	--
10	30	38.07	0.1230	0.0101	0.0552
11	60	39.11	0.1135	0.0086	0.0603

Table 14. Comparison of estimated to experimental results for D. E. Yake's model at 500°C and 30,000 psi compressed pellets

Run	Reaction time (min.)	Conversion ratio (%)	Calc. porosity (assume ε_o=0.35)	Calc. diffusivity from calc. porosity (cm^2/sec)	Experimental diffusivity (cm^2/sec)
1	0	0	0.3500	0.0822	0.0731
2	0.5	5.50	0.2885	0.0557	0.0416
3	1	7.33	0.2681	0.0481	0.0384
4	2	9.58	0.2429	0.0394	0.0342
5	3	13.72	0.1966	0.0258	--
6	3	17.74	0.1517	0.0153	0.0295
7	5	16.97	0.1603	0.0171	0.0287
8	10	21.10	0.1141	0.0087	0.0221
9	30	23.47	0.0876	0.0051	0.0226
10	60	29.29	0.0225	0.0003	0.0065
11	60	30.10	0.0135	0.0001	0.0089

XII. APPENDIX C:

COMPUTER PROGRAM FOR DIFFUSIVITY MEASUREMENT USING THE EXPERIMENTAL RESULT FROM DIFFUSION CELL

```
      COMPLEX X(0:63),Z(0:63)
      DIMENSION RX(0:63),YT(0:63),C(4),DP(4),P1(4)
      COMMON AA,BB,N,N2,III,M,DT,DF,A(3,3),B(3,3),P(4),E(0:63),
     CG(3,0:63),Z
      COMMON /DATA/LN,H1,H2,K1,K2
      COMMON/DINV/NS
      REAL LN,K1,K2
C     WRITE(6,101)
 101  FORMAT('      64,2,1')
      READ (5,*) RX,YT,DT,DF,N,N2,M,DELP,III
      READ (5,*) LN,H1,H2,K1,K2
      READ *,P,NS,QQ
      AA=-1.0
      BB=DT
      DO 10 I=0,N-1
 10   Z(I)=CMPLX(RX(I),0.)
      CALL FFT(Z)
      AA=1.0
      BB=DF
      KOUNT=0
 7    CALL EQUA
      T=0.0
      DO 2 I=0,N-1
C     WRITE (6,*),T,YT(I),E(I)
      T=T+DT
 2    E(I)=YT(I)-E(I)
      DO 9 I=NS,M
      DO 9 J=NS,M
      A(I,J)=0.0
      DO 9 K=0,N-1
 9    A(I,J)=A(I,J)+G(I,K)*G(J,K)
      PRINT *,' '
      PRINT *,' '
      CALL INV
      PRINT *,B
      DO 3 I=NS,M
      C(I)=0.0
      DO 3 J=1,N-1
 3    C(I)=G(I,J)*E(J)+C(I)
      DO 5 I=NS,M
      DP(I)=0.0
      DO 4 J=NS,M
 4    DP(I)=B(I,J)*C(J)+DP(I)
      P1(I)=P(I)
      P(I)=P(I)*EXP(DP(I))
      P(I)=QQ*P1(I)+(1.-QQ)*P(I)
 5    CONTINUE
      SUM=0.0
      DO 6 I=NS,M
 6    SUM=SUM+ABS(1.-1./EXP(DP(I)))
      KOUNT=KOUNT+1
```

```
      ERRSQ=0.0
      DO 8 I=0,N-1
8     ERRSQ=E(I)*E(I)+ERRSQ
      PRINT *,'KOUNT=',KOUNT
      PRINT *,'**************************************************
      PRINT *,'DP=',DP
      PRINT *,'PARAMETER=',P
      PRINT *,'SUM SQ.ERRORS=',ERRSQ
      PRINT *,'**************************************************
      IF(SUM.GT.DELP)GO TO 7
      P(2)=1./P(2)/P(2)
      P(3)=P(3)*P(3)
      PRINT *,'==========================================
     C==========='
      PRINT *,'=','DT=',P(1),'DE=',P(2),'EP=',P(3),'='
      PRINT *,'==========================================
     C==========='
      STOP
      END
      SUBROUTINE FFT(X)
      COMMON AA,BB,N,N2,III,M,DT,DF,A(3,3),B(3,3),P(4),E(0:63),
     CG(3,0:63),Z
      COMPLEX X(0:63),Y(0:63),W,Z(0:63)
      PI=3.1415927
4     GO TO (1,2)III
1     DO 10 J1=0,1
      DO 10 J2=0,1
      DO 10 J3=0,1
      DO 10 J4=0,1
      DO 10 J5=0,1
10    Y(J5+2*J4+4*J3+8*J2+16*J1)=X(J1+2*J2+4*J3+8*J4+16*J5)
      GO TO 3
2     DO 20 J1=0,1
      DO 20 J2=0,1
      DO 20 J3=0,1
      DO 20 J4=0,1
      DO 20 J5=0,1
      DO 20 J6=0,1
20    Y(J6+2*J5+4*J4+8*J3+16*J2+32*J1)=
     CX(J1+2*J2+4*J3+8*J4+16*J5+32*J6)
3     DO 30 L=0,N2-1
      L1=2**(N2-L)
      L2=2**(L)
      DO 30 K=0,N-1,L2*2
      DO 30 J=0,N/L1-1
      W=CEXP(CMPLX(0.,AA*PI*J*L1/N))
      Y(K+J)=Y(K+J)+Y(K+J+L2)*W
30    Y(K+J+L2)=Y(K+J)-2.*Y(K+J+L2)*W
      DO 90 I=0,N-1
90    X(I)=Y(I)*BB
      RETURN
```

```
      END
      SUBROUTINE INV
      COMMON AA,BB,N,N2,III,M,DT,DF,A(3,3),B(3,3),P(4),E(0:63),
     CG(3,0:63),Z
      COMPLEX Z(0:63)
      COMMON/DINV/NS
      DO 5 I=NS,M
      DO 5 J=NS,M
      B(I,J)=0.0
      IF(I.EQ.J) B(I,J)=1.0
5     CONTINUE
      DO 3 I=NS,M
      DIV=A(I,I)
      DO 1 J=NS,M
      A(I,J)=A(I,J)/DIV
1     B(I,J)=B(I,J)/DIV
      DO 2 J=NS,M
      IF(J.EQ.I) GO TO 2
      DIV=-A(J,I)
      DO 4 K=NS,M
      A(J,K)=DIV*A(I,K)+A(J,K)
4     B(J,K)=DIV*B(I,K)+B(J,K)
2     CONTINUE
3     CONTINUE
      RETURN
      END
      SUBROUTINE EQUA
      COMPLEX S,CA,CE(0:63),CG1(0:63),CG2(0:63),CG3(0:63),Z(0:63)
      COMPLEX S2,S3,S4,CSINH,CCOSH,CDEN,CI,TERM1,TERM2,CC
      REAL LN,K1,K2
      COMMON /DATA/LN,H1,H2,K1,K2
      COMMON AA,BB,N,N2,III,M,DT,DF,A(3,3),B(3,3),P(4),E(0:63),
     CG(3,0:63),Z
      PI=3.14159
      CI=CMPLX(1.,1.)
      CE(0)=(P(4)*K2/(P(2)*P(2)+K2+K1))*Z(0)
      CG1(0)=(0.,0.)
      CG2(0)=CE(0)*CE(0)/P(4)/K2*-2.*P(2)/Z(0)
      CG3(0)=(0.,0.)
      DO 1 I=1,N/2
      F=DF*I
      S=LN*SQRT(PI*F)*CI
      S2=S*S
      S3=S2*S
      S4=S3*S
      CC=CMPLX(0.,-2.*PI*F)
      CSINH=(CEXP(S*P(2)*P(3))-CEXP(-S*P(2)*P(3)))*.5
      CCOSH=CSINH+CEXP(-S*P(2)*P(3))
      TERM1=H1*H2*S4+(H1+H2+K1*K2/P(2)/P(2)*P(3)*P(3))*S2+1
      TERM2=(K1*H2+K2*H1)*S3+(K1+K2)*S
      CDEN=TERM1*P(2)/P(3)*CSINH+TERM2*CCOSH
```

```
      CE(I)=CEXP(CC*P(1))*P(4)*K2*S/CDEN*Z(I)
      CG1(I)=CE(I)*CC*P(1)
      CG2(I)=-CE(I)/CDEN*((TERM1-2.*K1*K2*P(3)*P(3)/P(2)/P(2)*S2)
     C/P(3)*CSINH+TERM1*P(2)*S*CCOSH+TERM2*P(3)*CSINH)*P(2)
      CG3(I)=-CE(I)/CDEN*((TERM1-2.*K1*K2*P(3)*P(3)/P(2)/P(2)*S2)
     C*-P(2)/P(3)/P(3)*CSINH+TERM1*P(2)*P(2)*S/P(3)*CCOSH+
     CTERM2*P(2)*S*CSINH)*P(3)
      CE(N-I)=CONJG(CE(I))
      CG1(N-I)=CONJG(CG1(I))
      CG2(N-I)=CONJG(CG2(I))
      CG3(N-I)=CONJG(CG3(I))
1     CONTINUE
      CALL FFT(CE)
      CALL FFT(CG1)
      CALL FFT(CG2)
      CALL FFT(CG3)
      DO 2 I=0,N-1
      E(I)=REAL(CE(I))
      G(1,I)=REAL(CG1(I))
      G(2,I)=REAL(CG2(I))
2     G(3,I)=REAL(CG3(I))
      RETURN
      END
```